bioRxiv preprint doi: https://doi.org/10.1101/2022.02.11.480120; this version posted February 14, 2022. The copyright holder for this preprint (which was not certified by peer review) is the author/funder, who has granted bioRxiv a license to display the preprint in perpetuity. It is made available under a CC-BY 4.0 International license.



# Residual force enhancement within the human quadriceps is greatest during submaximal stretch-hold contractions at a very long muscle length

Patrick Bakenecker[1], Tobias Weingarten[1], Daniel Hahn[1, 2] and Brent Raiteri[1]

[1]Human Movement Science, Faculty of Sport Science, Ruhr University Bochum, Germany

[2]School of Human Movement and Nutrition Sciences, University of Queensland, Brisbane, Australia

Address for correspondence:

Patrick Bakenecker

Ruhr-Universität Bochum

Gesundheitscampus Nord 10

44801 Bochum

Tel. +49 234 3222315

Fax +49 234 3214775

Email: patrick.bakenecker@rub.de

bioRxiv preprint doi: https://doi.org/10.1101/2022.02.11.480120; this version posted February 14, 2022. The copyright holder for this preprint (which was not certified by peer review) is the author/funder, who has granted bioRxiv a license to display the preprint in perpetuity. It is made available under a CC-BY 4.0 International license.




## Abstract

Little is known about how muscle length affects residual force enhancement (rFE) in humans. We therefore investigated rFE at short, long, and very long muscle lengths within the human quadriceps and patellar tendon (PT) using conventional dynamometry with motion capture ($rFE_{TQ}$) and a new, non-invasive shear-wave tensiometry technique ($rFE_{WS}$). Eleven healthy male participants performed submaximal (50% max.) EMG-matched fixed-end reference and stretch-hold contractions across these muscle lengths while muscle fascicle length changes of the vastus lateralis (VL) were captured using B-mode ultrasound. We found significant $rFE_{TQ}$ at long (7±5%) and very long (12±8%) but not short (2±5%) muscle lengths, whereas $rFE_{WS}$ was only significant at the very long (38±27%), but not short (8±12%) or long (6±10%) muscle lengths. We also found significant relationships between VL fascicle length and $rFE_{TQ}$ ($r$=0.63, $p$=.001) and $rFE_{WS}$ ($r$=0.52, $p$=.017), but relationships were not significant between VL fascicle stretch amplitude and $rFE_{TQ}$ ($r$=0.33, $p$=.126) or $rFE_{WS}$ ($r$=0.29, $p$=.201). PT shear-wave speed-angle relationships did not agree with estimated quadriceps muscle force-angle relationships, which indicates that estimating PT loads from shear-wave tensiometry might be inaccurate. We conclude that increasing muscle length rather than stretch amplitude contributes more to rFE during submaximal voluntary contractions of the human quadriceps.


Keywords: eccentric, force-length relation, knee extensors, muscle history dependence, shear wave tensiometry

bioRxiv preprint doi: https://doi.org/10.1101/2022.02.11.480120; this version posted February 14, 2022. The copyright holder for this preprint (which was not certified by peer review) is the author/funder, who has granted bioRxiv a license to display the preprint in perpetuity. It is made available under a CC-BY 4.0 International license.



## Introduction

Residual force enhancement (rFE) is a unique history-dependent property of skeletal muscle and is defined as the enhanced steady-state force following active muscle lengthening (i.e. stretch) relative to the steady-state force obtained during a fixed-end reference contraction at the same muscle length and level of activation (Edman et al. 1978; Cook and McDonagh 1995). rFE has been observed across muscle structural scales ranging from single sarcomeres (Leonard et al. 2010) or isolated fibres from animals (Abbott and Aubert 1952) or humans (Pinnell et al. 2019) to whole human muscles working *in vivo* (Cook and McDonagh 1995) during artificially-evoked or voluntary contractions (Lee and Herzog 2002; Seiberl et al. 2015).

*In vitro* experiments have shown that rFE is independent of stretch velocity (Edman et al. 1978; Tilp et al. 2009), but dependent on muscle length, whereby rFE is greater when the stretch ends at longer muscle lengths (Bullimore et al. 2007; Hisey et al. 2009). rFE generally increases with increasing stretch amplitude (Edman et al. 1978, 1982) until some critical amplitude on the descending limb of the force-length relationship (Bullimore et al. 2007; Hisey et al. 2009), but increasing stretch amplitude does not necessarily increase rFE when the stretch ends at shorter muscle lengths (Hisey et al. 2009). In comparison with *in vitro* experiments, stretch amplitude and muscle length are more difficult to control *in vivo*, primarily due to the multiple and relatively more compliant muscle-tendon units (MTUs) that cross a joint of interest, and their varying moment arms over a joint's range of motion that change with contraction intensity (Tsaopoulos et al. 2007). In a recent meta-analysis, de Campos et al. (2021) analysed how stretch amplitude affects *in vivo* rFE and concluded that rFE, which was estimated from resultant joint torques, was not dependent on stretch amplitude (i.e. the amount of joint rotation) during artificially-evoked or voluntary contractions. However, this review neglected the previously reported *in vitro* based interaction between stretch amplitude and muscle length on

bioRxiv preprint doi: https://doi.org/10.1101/2022.02.11.480120; this version posted February 14, 2022. The copyright holder for this preprint (which was not certified by peer review) is the author/funder, who has granted bioRxiv a license to display the preprint in perpetuity. It is made available under a CC-BY 4.0 International license.



rFE (Hisey et al. 2009), largely because very few *in vivo* studies have estimated the operating region of an individual muscle of interest on its force-length relationship.

*In vivo* experiments that have examined how muscle length affects rFE show somewhat conflicting results. Power et al. (2013) showed that rFE occurs at both short and long muscle lengths, whereas other studies found rFE only at long muscle lengths (Shim and Garner 2012; Fukutani et al. 2017; Bakenecker et al. 2020). One potential reason for the conflicting results could be that most studies tested at identical joint angles across participants for the different muscle length conditions, even though this could have resulted in rFE being examined only over the ascending *or* descending limb of the force-length relationship in some participants, and over both ascending *and* descending limbs in other participants. Consequently, it remains unclear how *in vivo* rFE is affected by muscle length.

Another difficulty with assessing the influence of muscle length on *in vivo* rFE is that muscle or tendon forces are typically estimated using net joint torque measurements and literature-based moment arms (Bakenecker et al. 2020). However, using literature-based moment arms might be inaccurate as moment arms can vary between individuals and genders (Nisell 1985), are affected by contraction intensity (Arampatzis et al. 2004; Tsaopoulos et al. 2007), and are influenced by the determination method (Bakenecker et al. 2019). Secondly, resultant joint torque measurements to infer rFE can be problematic because torque is influenced by (1) gravitational forces, (2) passive and active forces generated by agonistic and antagonistic muscles, and (3) misalignment between the joint axis of interest and dynamometer axis can occur (Arampatzis et al. 2004). These factors can make it difficult to validly quantify *in vivo* rFE and might be partly responsible for the discrepancies between *in vitro* and *in vivo* findings.

bioRxiv preprint doi: https://doi.org/10.1101/2022.02.11.480120; this version posted February 14, 2022. The copyright holder for this preprint (which was not certified by peer review) is the author/funder, who has granted bioRxiv a license to display the preprint in perpetuity. It is made available under a CC-BY 4.0 International license.



One potential solution to more directly quantify *in vivo* rFE involves using a new, non-invasive technique known as shear-wave tensiometry, which was introduced by Martin et al. (2018). These authors previously showed that the shear-wave propagation velocity in free tendons depends primarily on axial stress under physiological loads, and that *in vivo* tendon shear-wave speeds can be tracked by a shear-wave tensiometer, which consists of a skin-mounted tapping device and miniature accelerometers. The squared tendon shear-wave speeds measured with this device were shown to strongly correlate with joint torques during fixed-end knee extension and plantar flexion contractions (Martin et al. 2018). Squared Achilles and patellar tendon (PT) shear-wave speeds were also shown to strongly correlate with joint torques that were estimated using inverse dynamics during sections of the gait cycle (Martin et al. 2018). The usability of calibrated shear-wave tensiometers to assess *in vivo* Achilles tendon stress was later confirmed in experiments by the same group (Keuler et al. 2019).

Therefore, the aim of this study was to examine whether rFE is muscle-length dependent within the human quadriceps using conventional dynamometry and shear-wave tensiometry to estimate knee joint torques and PT loads, respectively. To achieve this aim, participants (N=16) performed submaximal voluntary EMG-matched (50% of the knee joint angle-specific maximum superficial quadriceps muscle activity) and rotation-amplitude-matched (15° knee joint rotation) stretch-hold and fixed-end reference contractions at short, long, and very long muscle lengths. To ensure that rFE was not influenced by differences in the muscle's isometric force capacity at short and long muscle lengths, we attempted to match PT loads at short and long muscle lengths. Based on the findings from *in vitro* experiments and the mechanisms predicted to contribute to greater rFE at longer muscle lengths, such as sarcomere length non-uniformities (Morgan 1990) and increased titin forces at longer muscle lengths (Flann et al. 2011), we hypothesised that rFE would increase with increasing muscle length rather than increasing stretch amplitude, which was partly verified by imaging muscle fascicle lengths and

bioRxiv preprint doi: https://doi.org/10.1101/2022.02.11.480120; this version posted February 14, 2022. The copyright holder for this preprint (which was not certified by peer review) is the author/funder, who has granted bioRxiv a license to display the preprint in perpetuity. It is made available under a CC-BY 4.0 International license.



length changes from one muscle, the vastus lateralis (VL), using B-mode ultrasound. We also expected a strong agreement (≥90%) between squared PT shear-wave speeds and the estimated force-length relationship of the quadriceps obtained during the submaximal voluntary fixed-end contractions.

bioRxiv preprint doi: https://doi.org/10.1101/2022.02.11.480120; this version posted February 14, 2022. The copyright holder for this preprint (which was not certified by peer review) is the author/funder, who has granted bioRxiv a license to display the preprint in perpetuity. It is made available under a CC-BY 4.0 International license.



## Results

*Exclusions*

Five participants did not complete the experiment because of problems with estimating their PT shear-wave speeds. No outliers in EMG, torque or VL fascicle length or length change data were detected from the remaining eleven participants. However, at the long muscle length, two outliers (4 median absolute deviations (MAD): 9316 $m^2s^{-2}$ [values: 29671 and 39375]) from the stretch-hold condition, and two outliers (4 MAD: 9544 $m^2s^{-2}$ [values: 22204 and 27710]) from the fixed-end reference condition were detected in the PT shear-wave-speed data. Consequently, the sample sizes for shear-wave-speed and $rFE_{WS}$ data for the short, long, and very long muscles lengths were 11, 9, and 11, respectively.

*Muscle activity levels*

A two-way repeated-measures ANOVA on the mean time-matched steady-state summed muscle activity level data from the superficial quadriceps muscles (VL, rectus femoris (RF), and vastus medialis (VM)) found a significant main effect of contraction condition ($F_{1,10}$ = 12.59, $p$ = .005). However, mean differences between stretch-hold and fixed-end reference contractions were within the allowed variation (<6% difference between the desired and recorded EMG levels) and not significant according to Sidak post-hoc comparisons at the short (-1.2% [95% CI: -3.4 to 1.0], $p$ = .396), long (-1.0% [95% CI: -2.9 to 0.8], $p$ = .367), and very long muscle lengths (-1.1% [95% CI: -2.2 to 0.1], $p$ = .076). There was no significant main effect of muscle length ($F_{1.53,15.26}$ = 0.05, $p$ = .914), and no significant interaction between contraction condition and muscle length ($F_{1.82,18.15}$ = 0.01, $p$ = .982). Mean time-matched steady-state biceps femoris muscle activity levels (n=7) during stretch-hold and fixed-end reference contractions were 4.6 ± 2.9% and 5.0 ± 3.3%, respectively. Descriptive statistics are reported in Table 1.

bioRxiv preprint doi: https://doi.org/10.1101/2022.02.11.480120; this version posted February 14, 2022. The copyright holder for this preprint (which was not certified by peer review) is the author/funder, who has granted bioRxiv a license to display the preprint in perpetuity. It is made available under a CC-BY 4.0 International license.



*Resultant knee extension torques*

Mean time-matched steady-state resultant knee extension torques during the stretch-hold and fixed-end reference contractions were 210.1 ± 48.6 Nm and 207.8 ± 53.1 Nm at the short muscle length, 253.7 ± 32.2 Nm and 236.0 ± 26.3 Nm at the long muscle length, and 210.8 ± 29.0 Nm and 189.0 ± 24.1 Nm at the very long muscle length. A two-way repeated-measures ANOVA on torque data revealed significant main effects of contraction condition ($F_{1,10}$ = 34.03, $p$ < .001) and muscle length ($F_{1.15,11.46}$ = 10.81, $p$ = .006), and a significant interaction between contraction condition and muscle length ($F_{1.99,19.85}$ = 7.96, $p$ = .003). Sidak post-hoc comparisons revealed no significant mean difference between the stretch-hold and fixed-end reference conditions at the short muscle length (2.4 Nm [95% CI: -5.8 to 10.5], $p$ = .813), but significant mean differences at the long (17.7 Nm [95% CI: 5.8 to 29.5], $p$ = .005) and very long muscle lengths (21.9 Nm [95% CI: 9.6 to 34.2], $p$ = .001).

*Patellar tendon shear-wave speeds*

Mean time-matched steady-state squared PT shear-wave speeds during the respective stretch-hold and fixed-end reference contractions were 3900 ± 2770 $m^2s^{-2}$ and 3677 ± 2703 $m^2s^{-2}$ at the short muscle length, 2872 ± 1179 $m^2s^{-2}$ and 2775 ± 1215 $m^2s^{-2}$ at the long muscle length, and 2601 ± 1554 $m^2s^{-2}$ and 1800 ± 846 $m^2s^{-2}$ at the very long muscle length. A two-way repeated-measures mixed-effects analysis on shear-wave-speed data revealed significant main effects of contraction condition ($F_{1,10}$ = 12.11, $p$ = .006) and muscle length ($F_{1.35,13.52}$ = 5.00, $p$ = .034), and a significant interaction between contraction condition and muscle length ($F_{1.69,13.51}$ = 4.63, $p$ = .034). Sidak post-hoc comparisons revealed no significant mean differences between the stretch-hold and fixed-end reference conditions at the short (223 $m^2s^{-2}$ [95% CI: -192 to 638], $p$ = .399) or long muscle lengths (97 $m^2s^{-2}$ [95% CI: -207 to 402], $p$ = .745), but a significant mean difference at the very long muscle length (802 $m^2s^{-2}$ [95% CI: 130 to 1473], $p$ = .020). Tukey post-hoc comparisons revealed that the mean differences in shear-wave speeds were only

bioRxiv preprint doi: https://doi.org/10.1101/2022.02.11.480120; this version posted February 14, 2022. The copyright holder for this preprint (which was not certified by peer review) is the author/funder, who has granted bioRxiv a license to display the preprint in perpetuity. It is made available under a CC-BY 4.0 International license.



significant during the fixed-end reference contractions between the short and very long (1878 $m^2s^{-2}$ [95% CI: 145 to 3610], $p = .034$) and long and very long muscle lengths (975 $m^2s^{-2}$ [95% CI: 81 to 1868], p = .034), but not significantly different between the short and long muscle lengths (903 $m^2s^{-2}$ [95% CI: -1197 to 3003], p = .471) or between muscle lengths during the stretch-hold contractions (overall: 270 to 1299 $m^2s^{-2}$, [95% CI: -871 to 2834], $p \geq .060$).

*Residual force enhancement*

$rFE_{TQ}$ values of 2 ± 5%, 7 ± 5% and 12 ± 8% were calculated at the short, long, and very long muscle lengths, respectively. $rFE_{WS}$ values at the same respective lengths were 8 ± 12%, 6 ± 10% and 38 ± 27%. A two-way repeated-measures mixed-effects analysis on rFE data revealed significant main effects of the rFE determination method ($F_{1,10} = 13.88$, $p = .004$) and muscle length ($F_{1.51,15.07} = 11.07$, $p = .002$), as well as a significant interaction between the rFE determination method and muscle length ($F_{1.39,12.49} = 9.43$, $p = .006$). Sidak post-hoc comparisons revealed rFE mean differences were not significant between resultant torque and shear-wave-speed methods at the short (-6% [95% CI: -15 to 3], $p = .248$) or long muscle lengths (2% [95% CI: -10 to 13], $p = .976$, but there was a significant difference between $rFE_{TQ}$ and $rFE_{WS}$ at the very long muscle length (-27% [95% CI: -8 to -45], $p = .006$). Individual results and descriptive statistics are shown in Figure 1A-B and Table 1, respectively.

bioRxiv preprint doi: https://doi.org/10.1101/2022.02.11.480120; this version posted February 14, 2022. The copyright holder for this preprint (which was not certified by peer review) is the author/funder, who has granted bioRxiv a license to display the preprint in perpetuity. It is made available under a CC-BY 4.0 International license.



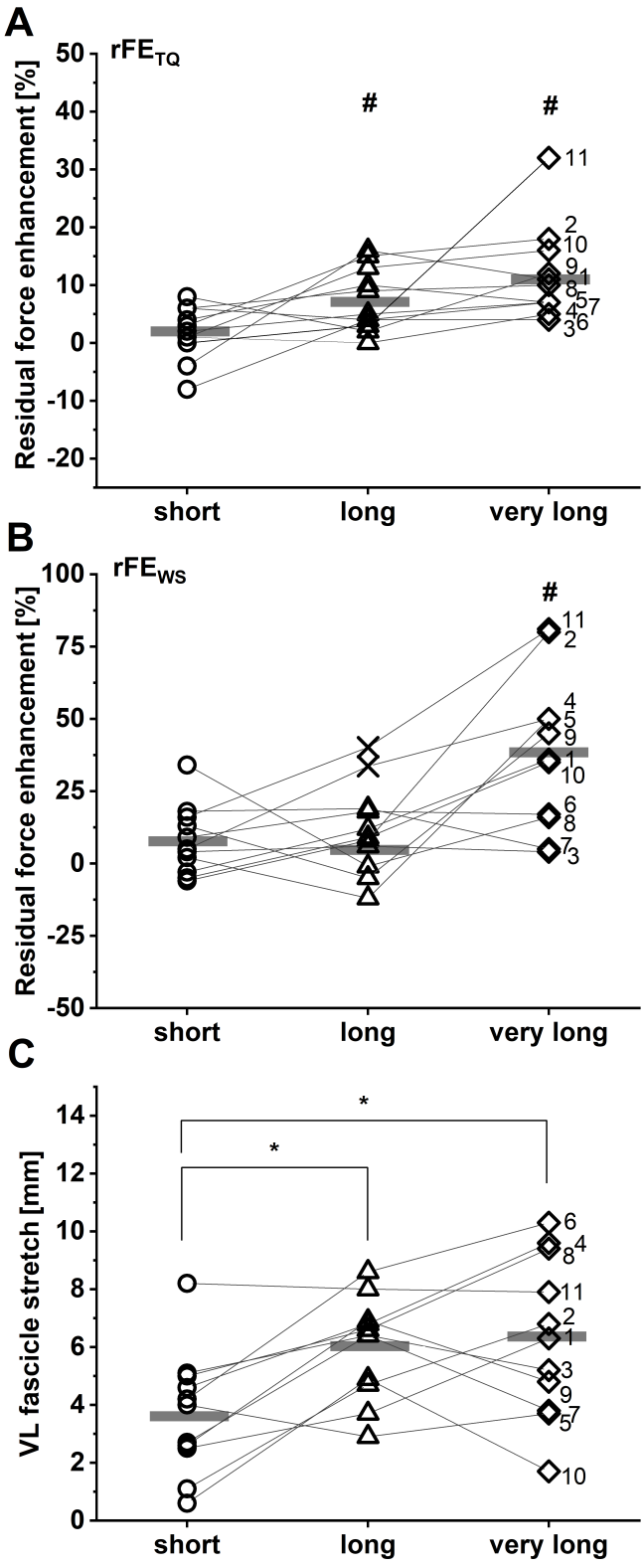



Figure 1. Individual and mean residual force enhancement magnitudes (n = 11) based on torque (A) and patellar tendon (PT) shear-wave speed recordings (B) at the short (dots), long (triangles) and very long (squares) muscle lengths. Individual and mean vastus lateralis (VL) muscle fascicle stretch amplitudes are shown in C (n = 11). Unfilled symbols represent the individual values and horizontal bars indicate the group mean for each condition.

bioRxiv preprint doi: https://doi.org/10.1101/2022.02.11.480120; this version posted February 14, 2022. The copyright holder for this preprint (which was not certified by peer review) is the author/funder, who has granted bioRxiv a license to display the preprint in perpetuity. It is made available under a CC-BY 4.0 International license.



Outliers that were excluded from analysis are indicated as an X in B (n = 2). Grey lines and black numbers distinguish between participants. *Indicates a significant difference between muscle length conditions ($P < 0.05$). #Indicates significant rFE for measures of resultant knee extension torques (A) and shear-wave speeds (B) ($P < 0.05$).

*Vastus lateralis muscle fascicle lengths and length changes*

During the stretch-hold contractions, VL muscle fascicles stretched by 3.7 ± 2.1 mm to the short muscle length, 6.0 ± 1.7 mm to the long muscle length, and 6.3 ± 2.8 mm to the very long muscle length. A one-way repeated-measures ANOVA revealed a significant main effect of muscle length on the magnitude of VL muscle fascicle stretch ($F_{1.86,18.57} = 9.10$, $p = .002$). Tukey post-hoc comparisons found significant mean differences in VL fascicle stretch between the short and long (-2.3 [95% CI: -3.9 to -0.7], $p = .007$), and short and very long muscle lengths (-2.6 mm [95% CI: -4.7 to -0.6], $p = .013$), but no significant mean difference between the long and very long muscle lengths (-0.3 mm [95% CI: -2.2 to 1.6], $p = .884$) (Figure 1C). No significant repeated-measures linear relationships were found between VL fascicle stretch amplitude and $rFE_{TQ}$ ($r = 0.33$, 95% CI: -0.12 to 0.67, $p = .126$) or $rFE_{WS}$ ($r = 0.29$, 95% CI: -0.19 to 0.66, $p = .201$) (Figure 2).

A two-way repeated-measures ANOVA on absolute VL muscle fascicle lengths revealed significant main effects of contraction condition ($F_{1,10} = 9.72$, $p = .011$) and fascicle length ($F_{1.98,19.78} = 46.56$, $p < .001$), and a significant interaction between contraction condition and fascicle length ($F_{1.98,19.76} = 5.09$, $p = .017$). Mean differences in fascicle length between stretch-hold and fixed-end reference contractions were significant according to Sidak post-hoc comparisons only at the long muscle length (-2 mm [95% CI: -3 to -1], $p = .002$), but not at the short (0 mm [95% CI: -1 to 2], $p = .961$) or very long muscle lengths (-1 mm [95% CI: -2 to 0], $p = .187$). Considering that the mean standard deviation and mean range of fascicle lengths for the fixed-end reference condition at the long muscle length was 2 mm and 4 mm across

bioRxiv preprint doi: https://doi.org/10.1101/2022.02.11.480120; this version posted February 14, 2022. The copyright holder for this preprint (which was not certified by peer review) is the author/funder, who has granted bioRxiv a license to display the preprint in perpetuity. It is made available under a CC-BY 4.0 International license.



participants, respectively, the significant difference in fascicle lengths between the stretch-hold and fixed-end reference contractions at the long muscle length is not likely to be meaningful as it falls within the measurement variability. Tukey post-hoc comparisons showed that the mean differences in absolute VL fascicle lengths were significant across the three muscle lengths for both contraction conditions (overall: 19 to 44 mm [95% CI: 8 to 56], $p \leq .003$). Significant repeated-measures linear relationships were found between absolute VL fascicle length (where mean fascicle lengths between the stretch-hold and fixed-end reference contractions were taken for each muscle length condition) and $rFE_{TQ}$ ($r = 0.63$, 95% CI: 0.27 to 0.83, $p = .001$), as well as absolute VL fascicle length and $rFE_{WS}$ ($r = 0.52$, 95% CI: 0.08 to 0.79, $p = .017$) (Figure 2).

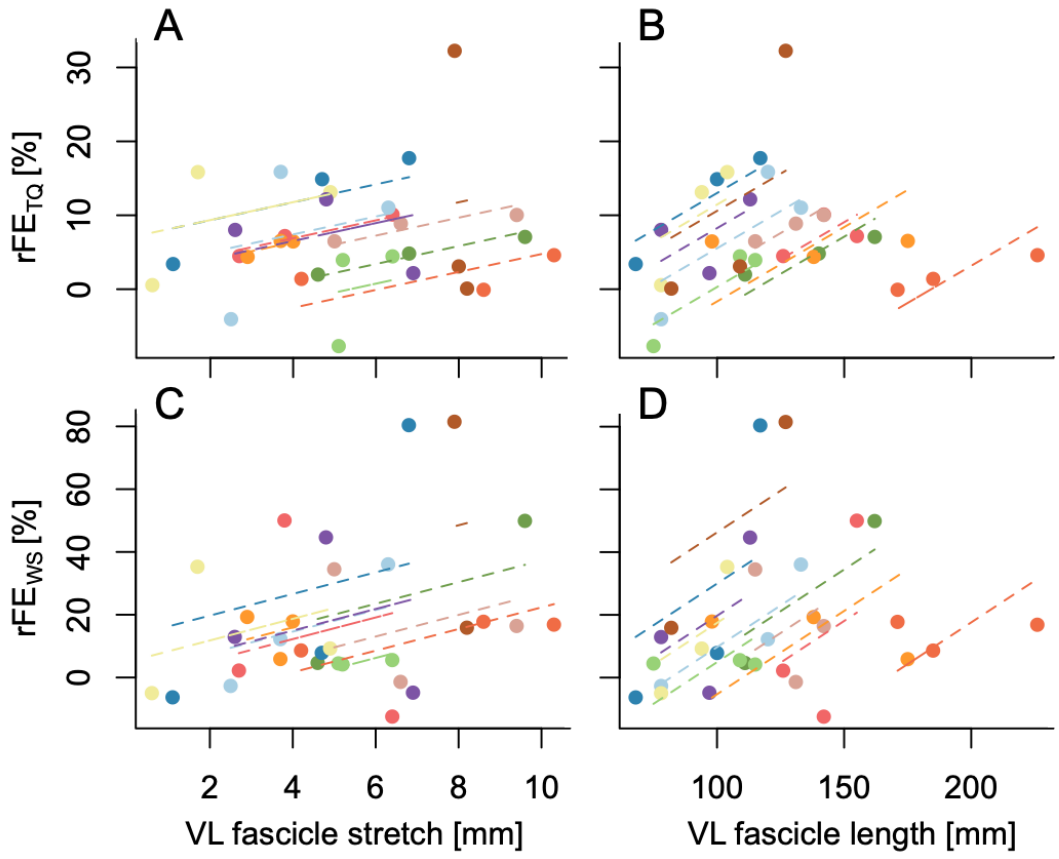



Figure 2. Repeated-measures linear relationships between $rFE_{TQ}$ and VL fascicle stretch amplitude (A: $r = 0.33$, 95% CI: -0.12 to 0.67, $p = .126$), $rFE_{TQ}$ and VL fascicle length (B: $r = 0.63$, 95% CI: 0.27 to 0.83, $p = .001$), $rFE_{WS}$ and fascicle stretch amplitude (C: $r = 0.29$, 95% CI: -0.19 to 0.66, $p = .201$), and $rFE_{WS}$ and VL fascicle length (D: $r = 0.52$, 95% CI: 0.08 to 0.79, p = .017).

bioRxiv preprint doi: https://doi.org/10.1101/2022.02.11.480120; this version posted February 14, 2022. The copyright holder for this preprint (which was not certified by peer review) is the author/funder, who has granted bioRxiv a license to display the preprint in perpetuity. It is made available under a CC-BY 4.0 International license.



*Kinematics*

The mean target knee joint angles determined from the optical motion analysis system for the fixed-end reference contractions were 28.2 ± 2.3°, 68.1 ± 10.1° and 83.6 ± 7.9° for the short, long, and very long muscle lengths, respectively. For the stretch-hold contractions, the mean target knee joint angles were 28.2 ± 4.3°, 68.7 ± 18.4° and 86.1 ± 19.2° for the short, long, and very long muscle lengths, respectively. During the stretch-hold contractions, the measured knee joint rotations during the amplitude-matched dynamometer-imposed rotations were 9.0 ± 4.3°, 14.7 ± 2.3° and 15.7 ± 2.8° to the short, long, and very long muscle lengths, respectively. The respective programmed dynamometer rotations were 14.8 ± 0.4°, 15.4 ± 0.4° and 15.2 ± 0.3°.

bioRxiv preprint doi: https://doi.org/10.1101/2022.02.11.480120; this version posted February 14, 2022. The copyright holder for this preprint (which was not certified by peer review) is the author/funder, who has granted bioRxiv a license to display the preprint in perpetuity. It is made available under a CC-BY 4.0 International license.



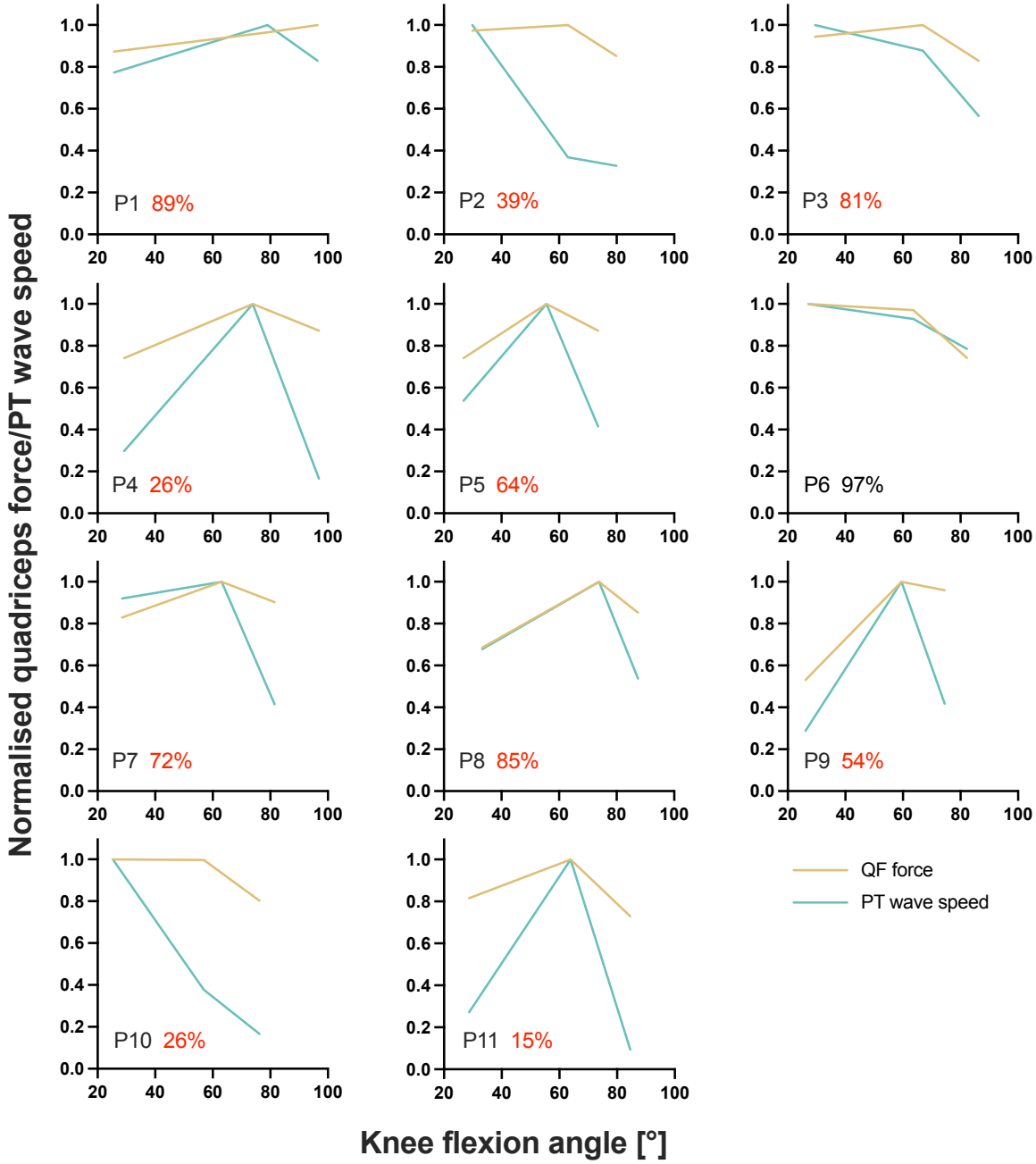



Figure 3. Individual normalised quadriceps-force-(QF)-angle and patellar tendon (PTws) shear-wave-speed-angle relationships determined from the fixed-end reference contractions at the short, long, and very long muscle lengths from part 2 of the experiment. The average agreement across muscle lengths (PTws – QF / mean of PTws and QF) between normalised QFs and PT shear-wave speeds is indicated as a percentage for every participant, where red font has been used to highlight instances of less than 90% agreement.

253 Table 1. Mean values and standard deviations for resultant knee extension torques, PT shear-wave speeds, normalized EMG amplitudes of the VL, VM, RF and their sum, as well
254 as VL fascicle length and fascicle stretch magnitudes during the stretch-hold contractions compared with the time-matched fixed-end contractions at the short, long, and very long
255 muscle lengths.

| Muscle length | short | | long | | very long | |
|---|---|---|---|---|---|---|
| Contraction condition | stretch-hold | fixed-end | stretch-hold | fixed-end | stretch-hold | fixed-end |
| Knee joint torque [Nm] | 210.1 ± 48.6 | 207.8 ± 53.1 | 253.7 ± 32.2* | 236.0 ± 26.3 | 210.8 ± 29.0* | 188.9 ± 24.1 |
| PT shear-wave speed $[ms^{-1}]^2$ | 3900 ± 2770 | 3677 ± 2703 | 2872 ± 1179 | 2775 ± 1215 | 2601 ± 1554* | 1800 ± 846 |
| VL EMG amplitude [% MVC] | 44.65 ± 5.78 | 45.35 ± 6.50 | 43.12 ± 4.19 | 43.62 ± 5.05 | 43.68 ± 5.70 | 43.38 ± 4.15 |
| VM EMG amplitude [% MVC] | 41.68 ± 5.25 | 44.04 ± 5.95 | 43.80 ± 4.84 | 43.50 ±4.26 | 42.70 ± 4.28 | 43.59 ± 4.21 |
| RF EMG amplitude [% MVC] | 51.60 ±10.86 | 52.53 ±10.60 | 48.86 ±8.66 | 52.12 ± 7.75 | 45.26 ± 6.98 | 48.44 ±8.19 |
| Summed EMG amplitude [% MVC] | 46.91 ± 2.35 | 48.08 ± 3.14 | 46.84 ± 2.06 | 47.86 ± 1.87 | 47.17 ± 3.30 | 48.22 ± 2.77 |
| VL fascicle length [mm] | 99 ± 34 | 99 ± 34 | 122 ± 24 | 124 ± 24 | 142 ± 36 | 143 ± 35 |
| VL fascicle stretch [mm] | 3.7 ± 2.1 | | 6.0 ± 1.8 | | 6.3 ± 2.8 | |

256 * Significantly different to fixed-end reference condition at $p < 0.05$. MVC, maximal voluntary contraction.

bioRxiv preprint doi: https://doi.org/10.1101/2022.02.11.480120; this version posted February 14, 2022. The copyright holder for this preprint (which was not certified by peer review) is the author/funder, who has granted bioRxiv a license to display the preprint in perpetuity. It is made available under a CC-BY 4.0 International license.



## Discussion

The main purpose of this study was to examine whether rFE magnitudes, which were estimated from resultant knee joint torques and PT shear-wave speeds during time- and EMG-matched submaximal stretch-hold and fixed-end reference contractions, are different at short, long, and very long muscle lengths. To our knowledge, this is the first *in vivo* experiment that has attempted to estimate rFE at more than two muscle lengths, and the first to use shear-wave tensiometry. We found that resultant knee extension torques were significantly higher during the steady-state phase of the stretch-hold compared with the fixed-end reference contractions at both the long and very long muscle lengths, whereas PT shear-wave speeds were significantly higher only at the very long muscle length. For both $rFE_{TQ}$ and $rFE_{WS}$ measures, we found the greatest rFE at the very long muscle length. Further, we found significant and strong positive repeated-measures relationships between absolute VL muscle fascicle length and $rFE_{TQ}$ and $rFE_{WS}$, but no significant repeated-measures relationships between VL muscle fascicle stretch amplitude and $rFE_{TQ}$ or $rFE_{WS}$. Taken together, $rFE_{TQ}$ and $rFE_{WS}$ findings indicate that *in vivo* rFE is maximised during submaximal voluntary contractions of the human quadriceps at a very long muscle length, and that *in vivo* rFE likely increases more with increasing muscle fascicle length than increasing fascicle stretch amplitude.

### *Resultant knee joint torques*

By using dynamometry and motion capture to calculate resultant net knee extension torques during submaximal stretch-hold and fixed-end reference contractions, we found significant $rFE_{TQ}$ at the long and very long muscle lengths, but not at the short muscle length (Figure 1A). This is in accordance to a previous study with a similar setup, where we also found significant rFE only at a long (10.7 ± 5.5%), but not at a short (1.3 ± 3.1%) muscle length (Bakenecker et al. 2020). Similar findings have been reported by Shim and Garner (2012) at short (no rFE) and long (4.7%) quadriceps muscle lengths. In contrast, Power et al. (2013) also found significant

bioRxiv preprint doi: https://doi.org/10.1101/2022.02.11.480120; this version posted February 14, 2022. The copyright holder for this preprint (which was not certified by peer review) is the author/funder, who has granted bioRxiv a license to display the preprint in perpetuity. It is made available under a CC-BY 4.0 International license.



283 rFE at short quadriceps muscle lengths (4–13%), but the rFE at long (7–20%) muscle lengths
284 was significantly higher. Unlike the aforementioned studies, which either tested at a common
285 knee flexion angle of 40° knee flexion or confirmed that the short muscle length was situated
286 on the ascending limb of the quadriceps torque-angle relationship, Power et al. (2013) tested at
287 60° knee flexion for their short muscle length condition, which would result in a longer muscle
288 length and therefore significant rFE based on our data (Figures 1 and 3).
289
290 *In vitro* findings suggest that rFE is not only muscle-length dependent, but also stretch-
291 amplitude dependent, where rFE generally increases with increasing stretch amplitude (Edman
292 et al. 1978, 1982) until some critical amplitude on the descending limb of the force-length
293 relationship (Bullimore et al. 2007; Hisey et al. 2009). As we observed no significant repeated-
294 measures linear relationship between VL fascicle stretch amplitude and $rFE_{TQ}$ (Figure 2), it is
295 unlikely that greater stretch amplitudes contributed to greater rFE at the long and very long
296 muscle lengths compared with the short muscle length. Based on the findings of Hisey et al.
297 (2009), where increasing stretch amplitude did not increase the amount of rFE at a target muscle
298 length 3 mm shorter than the muscle's optimal length for isometric force production, it is further
299 unlikely that greater stretch amplitudes to the short muscle length (i.e. on the ascending limb of
300 the force-length relationship) would have changed the rFE values we observed. In contrast to
301 *in vitro* findings on the descending limb of the force-length relationship (Hisey et al. 2009), a
302 recent meta-analysis by de Campos et al. (2021) suggested that rFE during *in vivo* experiments
303 is not affected by differences in stretch amplitude. Even though de Campos et al. (2021) simply
304 defined stretch amplitude based on the dynamometer-imposed rotation amplitude, this supports
305 our finding that *in vivo* rFE does not seem to be stretch-amplitude dependent. In contrast, we
306 found a significant and strong positive repeated-measures relationship between absolute VL
307 muscle fascicle length and $rFE_{TQ}$ (Figure 2). This is in accordance with *in vitro* experiments
308 that showed rFE increases with increasing muscle length (Bullimore et al. 2007; Hisey et al.

bioRxiv preprint doi: https://doi.org/10.1101/2022.02.11.480120; this version posted February 14, 2022. The copyright holder for this preprint (which was not certified by peer review) is the author/funder, who has granted bioRxiv a license to display the preprint in perpetuity. It is made available under a CC-BY 4.0 International license.



2009). Therefore, our torque measures support the idea that *in vivo* rFE is muscle-length dependent and not stretch-amplitude dependent. The increase in rFE with muscle length could potentially be due to a greater increase in stiffness of a passive elastic structure, such as titin (Rassier and Herzog 2005), as it is stretched to a very long muscle length.

*Shear-wave-speed measures*

By using shear-wave tensiometry to assess PT loads during submaximal stretch-hold and fixed-end reference contractions, we found significant $rFE_{WS}$ only at the very long muscle lengths, but not at the short or long muscle lengths (Figure 1B). Therefore, our findings are only partly in accordance with other *in vivo* findings that tend to show greater rFE values at long compared with short muscle lengths within the human quadriceps (Shim and Garner 2012; Power et al. 2013; Bakenecker et al. 2020) and plantar flexors (Pinniger and Cresswell 2007; Hahn et al. 2012; Fukutani et al. 2017; Hahn and Riedel 2018). With these previous findings in mind, we find it odd that $rFE_{WS}$ was prominent at the short muscle length (8%) even though the statistical analysis showed no significant difference in PT shear-wave speeds between stretch-hold and fixed-end contractions at this muscle length because of the $rFE_{WS}$ variability (12%). However, similar to rFE estimates based on resultant knee extension torques, we also found a significant and strong positive repeated-measures linear relationship between absolute VL muscle fascicle lengths and $rFE_{WS}$. This is in accordance with *in vitro* findings from the cat soleus muscle, where rFE increased from <2% to ~2-4% to ~6-14% as the target muscle length increased from 3 mm shorter to 3 mm and 9 mm longer than the muscle's optimal length for isometric force production (Hisey et al. 2009). Therefore, our shear-wave-speed measures also support the idea that *in vivo* rFE is muscle-length dependent.

In this study, we found rFE magnitudes based on resultant knee extension torques of 2±5%, 7±5% and 12±8% at the short, long, and very long muscle lengths, respectively. Based on PT

bioRxiv preprint doi: https://doi.org/10.1101/2022.02.11.480120; this version posted February 14, 2022. The copyright holder for this preprint (which was not certified by peer review) is the author/funder, who has granted bioRxiv a license to display the preprint in perpetuity. It is made available under a CC-BY 4.0 International license.



shear-wave speed measures, we observed rFE magnitudes of 8±12%, 6±10%% and 38±27% at the same respective lengths. Except for the $rFE_{WS}$ values at the very long muscle length, the rFE values from this study are in accordance with findings from the study of Seiberl et al. (2012), which also had participants perform submaximal voluntary stretch-hold and fixed-end reference contractions of the human quadriceps. At a similar crank arm angle (100° knee flexion) compared with what we used for the very long muscle length condition (104 ± 6°), Seiberl et al. (2012) observed rFE magnitudes of 7-11% and 3-5% at 30% and 60% of the maximum voluntary activity level, respectively. Other studies that investigated the human plantar flexors and the adductor pollicis showed similar rFE magnitudes (7-13%) during submaximal voluntary stretch-hold contractions (Oskouei and Herzog 2005, 2006; Pinniger and Cresswell 2007). rFE magnitudes greater than ~15% have only been found for electrically-stimulated human muscles (Cook and McDonagh 1995). The $rFE_{WS}$ values above 25% (see Figure 1B) we calculated might therefore be erroneous, which is supported by the much lower than expected normalised PT shear-wave speeds determined during the fixed-end reference contractions at the very long muscle length (see Figures 3 and 4). Unsurprisingly, the average agreement between normalised PT shear-wave speeds and estimated quadriceps' forces was worst at this muscle length (agreement at short: 72.4%; long: 81.5%; very long: 24.3%).

In general, obtaining plausible shear-wave speeds from the PT proved to be very difficult. In some of our participants (n=5), the shear-wave tensiometry technique resulted in unusable data, which is not that surprising, considering that Martin et al. (2018) also did not calculate shear-wave speeds from the PT during parts of the gait cycle (see their Supplementary Figure 6). For the remaining participants in the current study whose shear-wave speeds could be quantified, the accuracy of the measurements is questionable considering that we found an average agreement between squared PT shear-wave speeds and estimated quadriceps forces above 90% for one participant only (Figure 3 and Supplementary Figure 1). PT shear-wave-speed

bioRxiv preprint doi: https://doi.org/10.1101/2022.02.11.480120; this version posted February 14, 2022. The copyright holder for this preprint (which was not certified by peer review) is the author/funder, who has granted bioRxiv a license to display the preprint in perpetuity. It is made available under a CC-BY 4.0 International license.



measurements also became implausible during passive conditions where the MTU was at rest, during active conditions with stretch under high tension (Figure 4B), and during maximal voluntary contractions. Further, shear-wave speeds changed drastically across different joint angles, despite similar torque levels (Figure 4 B/E and C/F). Taken together, this indicates that quantifying PT loads can be problematic with shear-wave tensiometry and that the PT shear-wave speeds estimated by this technique might be inaccurate.

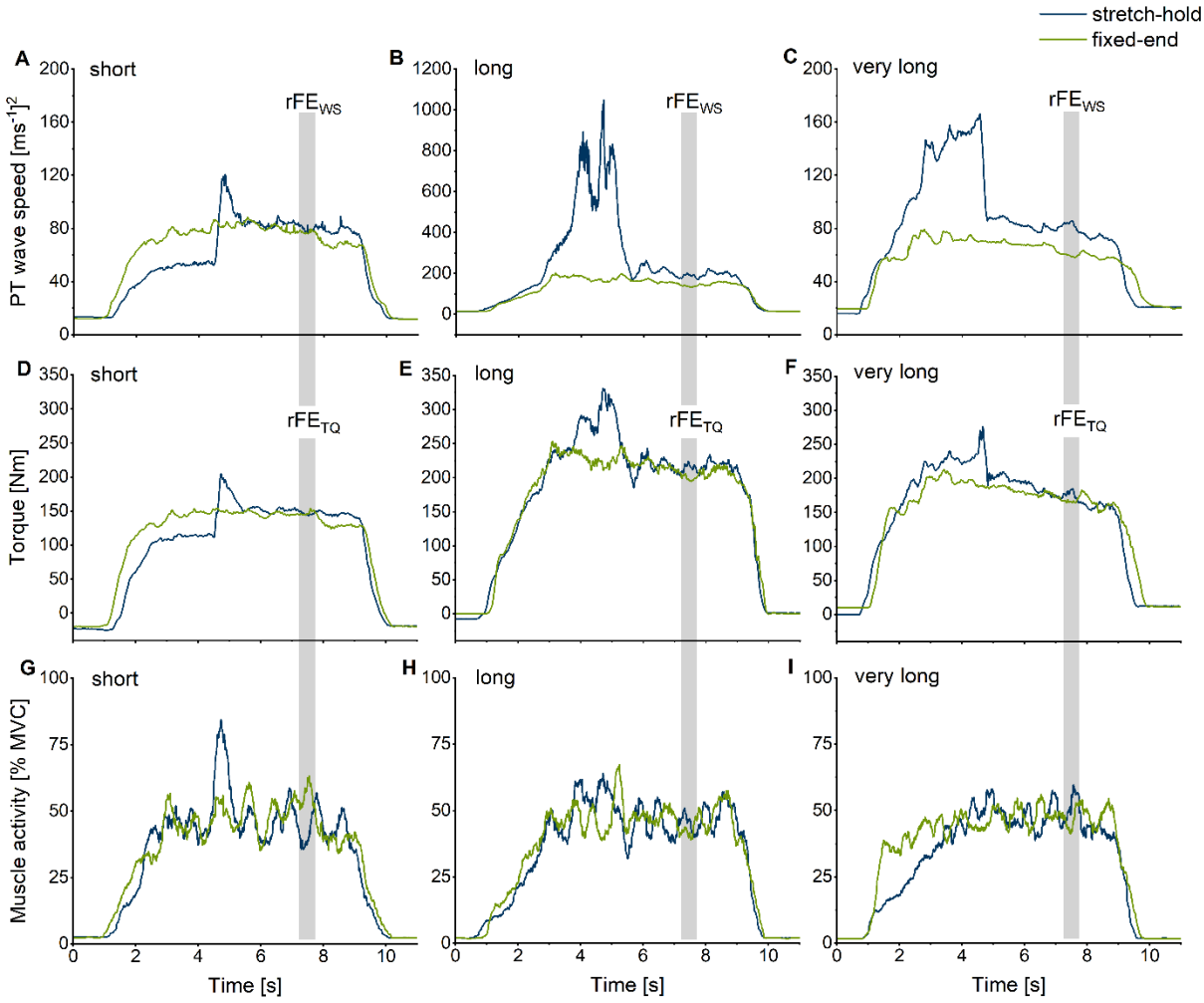



Figure 4. Exemplar (n = 1) patellar tendon (PT) shear-wave-speed-time (A, B, C), knee extension torque-time (D, E, F), and quadriceps muscle activity level-time traces (G, H, I) for the stretch-hold (blue) and fixed-end reference (green) contractions at the short (A, D, G), long (B, E, H), and very long (C, F, I) muscle lengths. The vertical grey shaded areas show the time intervals where mean PT shear-wave speeds and torques were analysed to evaluate $rFE_{WS}$ and $rFE_{TQ}$.

bioRxiv preprint doi: https://doi.org/10.1101/2022.02.11.480120; this version posted February 14, 2022. The copyright holder for this preprint (which was not certified by peer review) is the author/funder, who has granted bioRxiv a license to display the preprint in perpetuity. It is made available under a CC-BY 4.0 International license.



The main assumption of shear-wave tensiometry is that the shear-wave propagation speed depends primarily on tendon axial stress under physiological loads (Martin et al. 2018). Even if this assumption holds true, which might not be the case under very low or high physiological loads (Sarvazyan et al. 2013; Blank et al. 2022), axial stress is influenced by both the force in the tendon and the tendon's architecture (i.e. the width and thickness of the tendon). A recent study by Martin et al. (2020) suggests that the calibration gain required to estimate tendon stress based on tendon shear-wave speed appears to increase with increasing tendon aspect ratios (i.e. increasing tendon width relative to tendon thickness). Accordingly, when the tendon's architecture changes (e.g., through deformation of the tendon due to an applied stress) (Kuervers et al. 2021) under different contraction conditions (e.g., during a stretch-hold contraction that covers different joint angles and contraction intensities), shear-wave speeds could vary at the same tendon stress. Thus, shear-wave speeds may not accurately reflect tendon stress unless the changes in tendon architecture are accounted for. The accuracy of the shear-wave-speed measures might also depend on the amount of stress that is applied to the tendon. In former studies (Martin et al. 2018; Keuler et al. 2019), high correlations between squared shear-wave speed ($\leq$80 $m^2s^{-2}$) and torque measures ($\leq$200 Nm) were found when muscle activities and corresponding tendon stresses were low during preferred-speed walking ($\leq$50 MPa). In contrast, under the higher resultant knee extension torques (112-296 Nm) and presumably higher tendon stresses (>50 MPa) at the submaximal muscle activity levels that were used in this study, the estimated force-angle relationships were not reflected by the shear-wave-speed measures (Figure 3). Additionally, shear-wave-speed estimates became unreasonable when participants increased their activation level during the maximum voluntary contractions from the first part of the experiment (Supplementary Figure 2). Therefore, high tendon stresses and changing tendon dimensions might be problematic for accurately estimating PT tendon loads based on shear-wave-speed measures.

bioRxiv preprint doi: https://doi.org/10.1101/2022.02.11.480120; this version posted February 14, 2022. The copyright holder for this preprint (which was not certified by peer review) is the author/funder, who has granted bioRxiv a license to display the preprint in perpetuity. It is made available under a CC-BY 4.0 International license.



*Non-responders*

Previous *in vivo* experiments that examined rFE during voluntary contractions have identified a number of participants not showing rFE (Oskouei and Herzog 2006; Hahn et al. 2007, 2012; Tilp et al. 2009). These participants were subsequently called non-responders. We also found instances where participants did now show enhanced torques and/or enhanced PT shear-wave speeds during the stretch-hold compared with the fixed-end reference contractions. However, in opposition to the idea of there being a true non-responder, there was no participant in our dataset who consistently showed no rFE across the three muscle lengths we tested. We therefore speculate that there is no true non-responder. This speculation is supported by recent work from Paternoster et al. (2021), who showed that voluntary rFE appeared inconsistently in the same participants across five testing sessions, whereas during submaximal tetanic electrical muscle stimulation, all subjects consistently showed rFE. Indeed, having participants match muscle activity levels through voluntary effort, rather than through artificial stimulation, likely adds variability to rFE estimates (especially over a short duration analysis window like the one used here), and might contribute to the 'non-responder' phenomenon.

Limitations

Although we performed EMG feedback-controlled contractions to ensure the same level of superficial quadriceps activity during stretch-hold and fixed-end reference contractions and we assessed VL muscle fascicle stretch magnitudes, our rFE values could be influenced by different preloads prior to the stretch phase of the stretch-hold contractions at the short, long, and very long muscle lengths. Due to the relatively high compliance of human lower limb MTUs, using a preload prior to a stretch-hold contraction at the MTU level results in shortening-isometric-stretch-isometric muscle fascicle behavior, where the initial shortening of muscle fascicles increases with an increasing preload or a shorter initial muscle length. As rFE can be influenced by the amount of shortening preceding stretch (Lee et al. 2001) and active shortening can cause

bioRxiv preprint doi: https://doi.org/10.1101/2022.02.11.480120; this version posted February 14, 2022. The copyright holder for this preprint (which was not certified by peer review) is the author/funder, who has granted bioRxiv a license to display the preprint in perpetuity. It is made available under a CC-BY 4.0 International license.



residual force depression (i.e. a reduction in the steady-state isometric force following shortening (Abbott and Aubert 1952; Granzier et al. 1989)), differences in muscle fascicle shortening across the three tested muscle lengths could have influenced the estimated rFE magnitudes. Further, we only assessed stretch amplitudes and muscle fascicle lengths from a limited region within the VL muscle and we needed to perform linear extrapolation to estimate fascicle lengths, so we recommend that future studies investigate a muscle with shorter and less curved fascicles to better evaluate the influence of stretch amplitude and fascicle length on rFE.

## Conclusion

The purpose of this study was to investigate whether *in vivo* rFE within the human quadriceps varies with muscle length. We therefore investigated rFE within the human quadriceps and PT at short, long, and very long muscle lengths by respectively using conventional dynamometry and motion analysis ($rFE_{TQ}$) and a new, non-invasive technique known as shear-wave tensiometry ($rFE_{WS}$). We found significant $rFE_{TQ}$ at the long (7±5%) and very long (12±8%) muscle lengths, but not at the short (2±5%) muscle length, whereas $rFE_{WS}$ was only significant at the very long (38±27%) muscle length, but not at the short (8±12%) or long (6±10%) muscle lengths. We also found significant and strong positive repeated-measures relationships between absolute VL muscle fascicle length and $rFE_{TQ}$ and $rFE_{WS}$, but no significant relationships were observed between VL muscle fascicle stretch amplitude and $rFE_{TQ}$ or $rFE_{WS}$. We therefore conclude that increasing muscle length, rather than increasing stretch amplitude, contributes more to *in vivo* rFE during submaximal voluntary contractions of the human quadriceps. Further, the accuracy of PT shear-wave speeds estimated by shear-wave tensiometry is questionable as evidenced by low agreement (59% on average) between PT shear-wave speed-angle relationships and estimated quadriceps muscle force-angle relationships, as well as greater variability of $rFE_{WS}$ estimates compared with $rFE_{TQ}$ estimates (10-27% and 5-8% variability, respectively).

bioRxiv preprint doi: https://doi.org/10.1101/2022.02.11.480120; this version posted February 14, 2022. The copyright holder for this preprint (which was not certified by peer review) is the author/funder, who has granted bioRxiv a license to display the preprint in perpetuity. It is made available under a CC-BY 4.0 International license.



## Material and Methods

### Participants

Sixteen healthy males gave free written informed consent prior to participating in the study, eleven of whom (age 28.4 ± 5.9 years; height 187.1 ± 5.8 cm; weight 82.8 ± 8.0 kg) had data that could be analysed as their PT tendon shear-wave speeds could be quantified. All participants were free of knee injuries and neuromuscular disorders. All experimental procedures were approved by the local Ethics Committee of the Faculty of Sport Science at Ruhr University Bochum and conformed with the Declaration of Helsinki.

### Experimental protocol

The entire experiment consisted of one familiarization session and one test session. Familiarization helped participants to become comfortable with the dynamometer and improved their ability to perform maximum voluntary contractions (MVCs) and EMG-matched stretch-hold and fixed-end contractions. Each experimental session started with a standardised warm-up that included 10-15 submaximal knee extensions (~50-80% of perceived maximum effort) to precondition the MTU (Maganaris et al. 2002). MVCs were performed with standardized verbal encouragement from the investigator, while participants received real-time visual feedback of their knee joint torque (Gandevia 2001). During EMG-controlled contractions, participants received real-time (250 ms delay) visual feedback of their 500 ms moving root-mean-square (RMS) knee extensor muscle activity amplitude (i.e. muscle activities of VL, VL and RF were summed), which they attempted to visually match within predefined EMG/muscle activity ramps that were 5% apart.

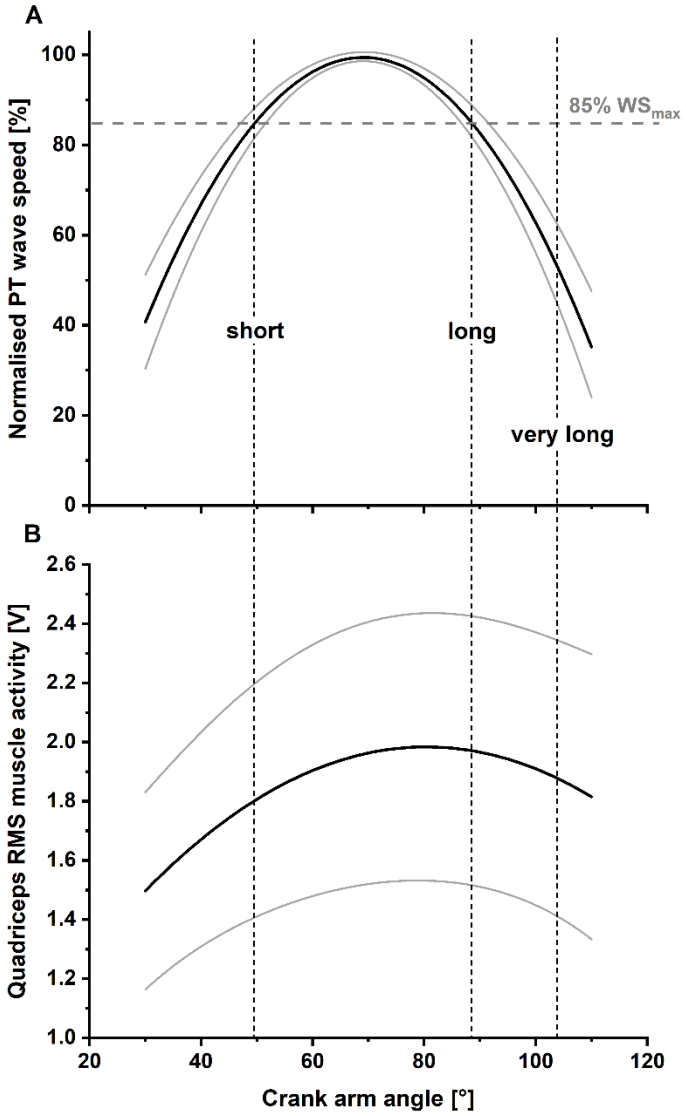
#### *Test session part 1 – Determination of the shear-wave-speed-angle relationship*

Participants' individual shear-wave-speed-angle relationships were first determined to ensure that the stretch-hold and corresponding fixed-end reference contractions during the second part

bioRxiv preprint doi: https://doi.org/10.1101/2022.02.11.480120; this version posted February 14, 2022. The copyright holder for this preprint (which was not certified by peer review) is the author/funder, who has granted bioRxiv a license to display the preprint in perpetuity. It is made available under a CC-BY 4.0 International license.



of the experiment were performed at short (i.e. ascending limb of the F-l-r), long, and very long (i.e. both on the descending limb of the F-l-r) muscle lengths. To determine the shear-wave-speed-angle relationship, participants performed maximum voluntary knee extension contractions at 30°, 70°, and 110° crank arm angles (Figure 5). Subsequently, participants performed EMG-controlled ramp contractions from rest to 50% of their angle-specific maximum muscle activity at the same crank arm angles. Participants were instructed to build up to the required 50% muscle activity level over a period of 3 s and then to hold this level for another 2 s. To minimize fatigue, participants received at least three and two minutes of rest between maximum voluntary contractions and submaximal contractions, respectively.



bioRxiv preprint doi: https://doi.org/10.1101/2022.02.11.480120; this version posted February 14, 2022. The copyright holder for this preprint (which was not certified by peer review) is the author/funder, who has granted bioRxiv a license to display the preprint in perpetuity. It is made available under a CC-BY 4.0 International license.



Figure 5. Solid lines indicate the mean normalized fitted patellar tendon (PT) shear-wave-speed-angle relationship (Panel A) and mean fitted quadriceps muscle activity-angle relationship (Panel B) across all participants (N = 11) with lower and upper 95% confidence intervals (dashed lines). Two different knee joint angles (i.e. the short and long muscle lengths), with a matched PT shear-wave speed capacity (85% of maximum PT shear-wave speed), were selected as the target knee joint angles for the stretch–hold and fixed-end reference contractions. A third target knee joint angle, referred to as the 'very long muscle length', was defined as a crank arm angle 15° more flexed than the crank arm angle at the long muscle length.

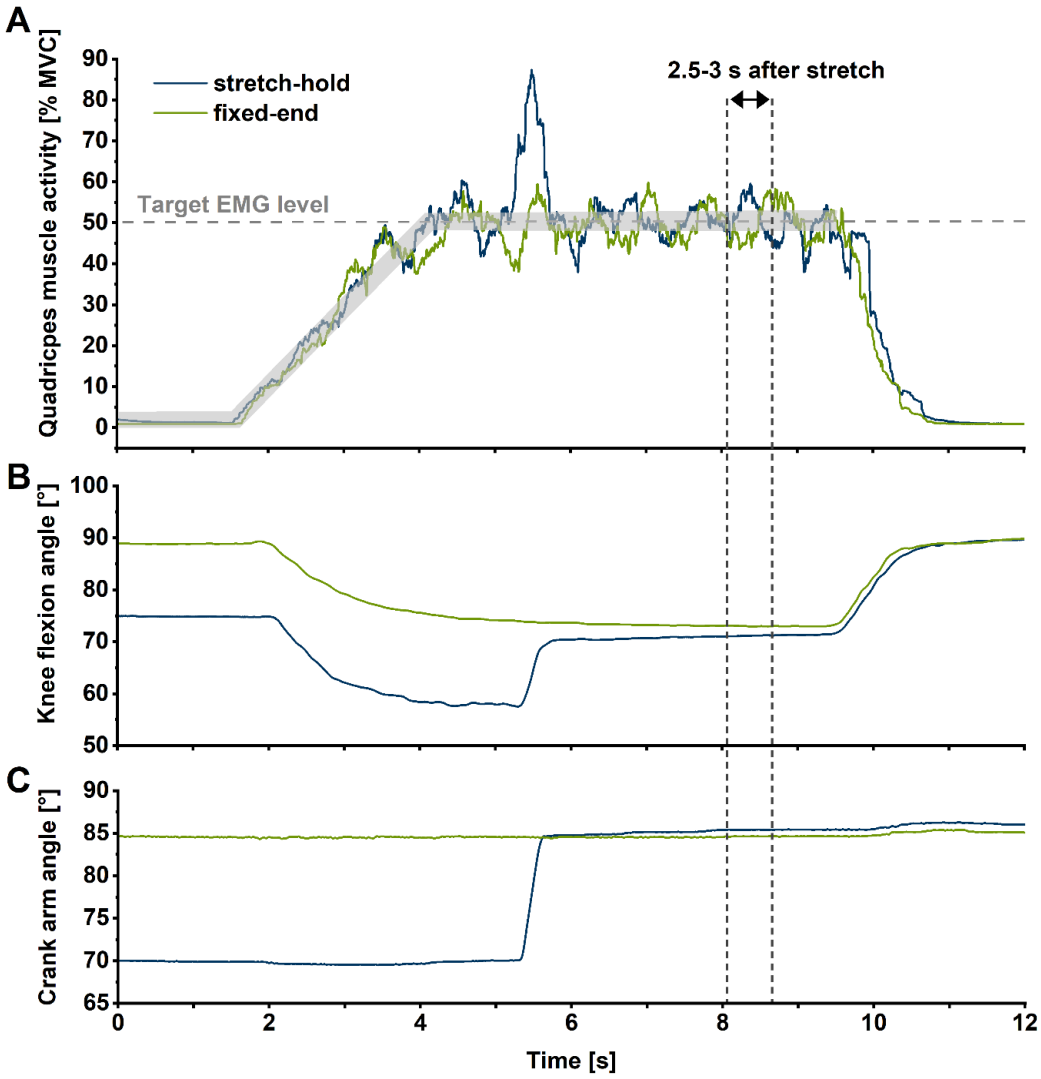
*Test session part 2 – Determination of residual force enhancement at short, long, and very long muscle lengths*

Using the submaximal (50% of maximal activity) shear-wave-speed-angle relationship determined in part 1, one knee joint angle on both sides of the plateau of the shear-wave-speed-angle relationship with the same PT shear-wave speed (i.e. 85% of the maximum recorded shear-wave speed) was selected as the reference knee joint angle for the fixed-end contractions at short and long muscle lengths. An additional fixed-end reference contraction was performed at a knee joint angle that was 15° more flexed than the joint angle at the long muscle length (which is referred to as the 'very long muscle length'). Stretch-hold contractions to the short, long, and very long muscle lengths were performed with a 15° crank arm rotation amplitude to the predetermined knee joint angle for each muscle length condition. The hold phase of the stretch-hold contractions was 6 s, which allowed rFE to be determined (Figures 4 and 6). The crank arm rotation velocity was set to $60°s^{-1}$ and was triggered 1.5 s after participants reached the plateau of the required muscle activity level. Similar to part 1, participants were asked to ramp up their muscle activity level and hold it at 50% of their angle-specific maximum muscle activity level during stretch-hold and fixed-end contractions (Figure 6A). The two contraction types were performed at least three times each in a randomised order and participants received at least two minutes of rest between contractions. At the end of the session, participants performed a maximum knee flexion contraction at a 70° crank arm angle, and the maximum

bioRxiv preprint doi: https://doi.org/10.1101/2022.02.11.480120; this version posted February 14, 2022. The copyright holder for this preprint (which was not certified by peer review) is the author/funder, who has granted bioRxiv a license to display the preprint in perpetuity. It is made available under a CC-BY 4.0 International license.



514 EMG activity amplitude was used to normalize the biceps femoris muscle activity level during
515 the stretch-hold and fixed-end reference knee extension contractions.




516

517 Figure 6. Exemplar (n = 1) summed superficial quadriceps muscle activity level-time (A), knee flexion angle-time
518 (B), and crank arm angle-time traces during stretch-hold (blue line) and fixed-end reference (green line)
519 contractions at the long muscle length. For every muscle length condition, participants were instructed to match
520 their quadriceps muscle activity level (calculated as a 250 ms centered root-mean-square amplitude) to a predefined
521 trace that ramped up to 50% of their angle-specific maximum over 3 s during both stretch-hold and fixed-end
522 reference contractions. Outcome measures were analysed in the time interval from 2.5 to 3 s after stretch (vertical
523 dotted lines), which corresponded to ~6 s after contraction onset in the stretch-hold and fixed-end reference
524 contractions.

525

bioRxiv preprint doi: https://doi.org/10.1101/2022.02.11.480120; this version posted February 14, 2022. The copyright holder for this preprint (which was not certified by peer review) is the author/funder, who has granted bioRxiv a license to display the preprint in perpetuity. It is made available under a CC-BY 4.0 International license.



Experimental Setup

Participants performed knee extension contractions with their right leg while sitting in a reclined position (100° hip flexion) on the seat of a motorized dynamometer (IsoMed2000, D&R Ferstl, GmbH, Hemau, GER). The participants' right lower leg was fixed with Velcro around the mid-shank to a cushioned attachment that was connected to the crank arm of the dynamometer. Two shoulder restraints and one waist strap were used to secure participants firmly in the seat of the dynamometer. Participants folded their arms across their chest prior to each contraction to limit accessory movements. To compensate for the knee joint rotation that occurs during activation of the quadriceps (Arampatzis et al. 2004; Bakenecker et al. 2019), the knee joint and the dynamometer axis of rotation were aligned during an active contraction of the quadriceps at every final knee joint position tested (i.e. corresponding to the short, long, and very long muscle lengths).

Torque measurements

The dynamometer was used to measure crank arm angle and knee joint torque during stretch-hold and fixed-end contractions. Torque and crank arm angle data were sampled at 2 kHz and synchronised using a 16-bit Power 1401 and Spike2 data collection system (Cambridge Electronic Design, UK).

Patellar tendon shear-wave speed

In line with Martin et al. (2018), we determined PT shear-wave speed using a piezo-actuated tapper that delivered micron-scale impulses through the skin over the PT, which induced a transient shear wave (i.e. a transverse motion of the tendon) that was detected by two adjacent miniature accelerometers. The mechanical tapping device was built as described in Martin et al. (2018). The tapper had a lever arm of 10 mm and its axis of rotation was secured over the PT using adhesive bandage. The 16-bit Power 1401 produced a square-wave pulse sequence

bioRxiv preprint doi: https://doi.org/10.1101/2022.02.11.480120; this version posted February 14, 2022. The copyright holder for this preprint (which was not certified by peer review) is the author/funder, who has granted bioRxiv a license to display the preprint in perpetuity. It is made available under a CC-BY 4.0 International license.



(0.5–9.5 V, 50% duty cycle, 50 Hz repetition rate) that was amplified by an open-loop piezo controller (MDT694B, Thorlabs) used to drive the tapper. Transient shear waves were induced in the PT by both extension and retraction of the actuator, but shear-wave speeds were derived only from the extension of the actuator, which resulted in 50 Hz shear-wave speed data.

The transverse motion of the PT was measured at two points using single-axis accelerometers (PCB-352A26, PCB Synotech, Germany) with 10 mV/g sensitivity. The miniature (8.6 × 4.1 × 2.8 mm, 0.2 g) accelerometers were secured in tight-fitting silicon housings and strapped over the PT using adhesive tape. The first accelerometer was positioned approximately 5 mm proximal to the tapper. The inter-accelerometer distance (center-to-center) was 9 mm and accelerometer signals were sampled at 100 kHz using the Spike2 data collection system. PT shear-wave speed was calculated following each contraction using Python and the steps previously described in Martin et al. (2018).

Knee joint kinematics

Due to soft tissue deformation and dynamometer compliance during voluntary contractions (Arampatzis et al. 2004), knee joint angles (can) differ from the crank arm angle of the dynamometer. We therefore determined the actual knee joint angles across contraction conditions using an optical motion analysis system (Optitrack, Natural Point, OR, USA) with four cameras. Three reflective markers were positioned on the cushioned attachment that was connected to the crank arm of the dynamometer (i.e. the mid-shank), with one marker each on the most prominent points of the lateral and medial femoral epicondyles, and on the line between the greater trochanter and the lateral femoral condyle. To determine potential misalignment of the knee joint axis and the dynamometer axis, three additional markers were placed on the dynamometer, with one marker over the dynamometer axis. Data was sampled at

bioRxiv preprint doi: https://doi.org/10.1101/2022.02.11.480120; this version posted February 14, 2022. The copyright holder for this preprint (which was not certified by peer review) is the author/funder, who has granted bioRxiv a license to display the preprint in perpetuity. It is made available under a CC-BY 4.0 International license.



100 Hz using Motive software (version 2.2, Natural Point, OR, USA) and synchronised with all other data by a common digital pulse.

Surface Electromyography

Surface EMG (NeuroLog System NL905, Digitimer Ltd, UK) was used to record the muscle activities of the vastus lateralis (VL), rectus femoris (RF), vastus medialis (VM) and biceps femoris of the right leg. After skin preparation (i.e. shaving, abrading and swabbing the skin with antiseptic), two surface electrodes (8 mm recording diameter, Ag/AgCl, Kendall H124SG, Massachusetts, USA) were placed over these muscles according to SENIAM guidelines (Hermens et al. 2000) using a 2 cm inter-electrode distance. Due to the placement of the ultrasound transducer, electrodes were placed towards the distal end of VL's mid belly. A single reference electrode was secured over the fibular head of the left leg. EMG signals were band-pass filtered between 0.01-20 kHz and amplified 2000 times (NL844, Digitimer Ltd, UK), before being sampled at 2 kHz using the Spike2 data collection system.

Ultrasound Imaging

To image the muscle fascicles of VL during stretch-hold and fixed-end contractions, a PC-based ultrasound system (LogicScan 128 CEXT-1Z Kit, Telemed, Vilnius, Lithuania) was used, which was connected to a flat-sided 96-element transducer (LV7.5/60/96, B-mode, 8.0 MHz, 60 mm depth; Telemed, Vilnius, Lithuania). The transducer captured images at 150 Hz and was placed over the mid-belly of VL (Sharifnezhad et al. 2014). The location of the transducer on the skin was secured using a custom 3D-printed plastic frame and adhesive bandage. The ultrasound system generated a digital pulse that was used to synchronize all digital signals to a common start and end time.

Data analysis

bioRxiv preprint doi: https://doi.org/10.1101/2022.02.11.480120; this version posted February 14, 2022. The copyright holder for this preprint (which was not certified by peer review) is the author/funder, who has granted bioRxiv a license to display the preprint in perpetuity. It is made available under a CC-BY 4.0 International license.



All data processing and analysis were performed using custom-written scripts in Python. Torque and crank arm angle data were filtered using a dual-pass fourth-order 20 Hz low-pass Butterworth filter. The knee angle was determined as the dihedral angle between the planes of the three markers on the shank and thigh. EMG signals from the superficial quadriceps muscles (VL, RF, VM) and the biceps femoris muscle were smoothed using a centred moving root-mean-square (RMS) amplitude calculation of 250 ms. Calculated shear-wave speed was squared. Fascicle length data were calculated using filtered x-y fascicle endpoint coordinates, which were filtered with a dual-pass second-order 6 Hz low-pass Butterworth filter. Only trials that had less than 6% difference between the predefined angle-specific EMG target level and measured knee extensor EMG level were included in the analysis (Raiteri and Hahn 2019).

*Resultant torque*

To account for potential over- or underestimation of the knee joint torque due to misalignment between the knee joint axis and the dynamometer axis, we recalculated knee joint torque as follows. The point of force application by the shank was assumed to be at the centre of the cushioned pad attached to the shank. From this centre point, the lever arm of the dynamometer crank arm was measured as the shortest perpendicular distance to the axis of rotation of the dynamometer. The lever arm of the shank was measured as the perpendicular distance between the knee joint centre (assumed to be halfway between the medial and lateral femoral epicondyles) and the centre of the cushioned shank pad. Furthermore, the dihedral angle between the crank arm and the shank was determined (see Supplementary Figure 3). The resultant torque was calculated by first finding the force at the centre of the cushioned shank pad through division of the measured peak-to-peak torque by the dynamometer lever arm. This force was then divided by the cosine of the angle between the crank arm and shank to find the force that was applied perpendicular to the shank. Resultant torque was then this corrected force times the lever arm of the shank.

bioRxiv preprint doi: https://doi.org/10.1101/2022.02.11.480120; this version posted February 14, 2022. The copyright holder for this preprint (which was not certified by peer review) is the author/funder, who has granted bioRxiv a license to display the preprint in perpetuity. It is made available under a CC-BY 4.0 International license.



629

630 *Shear-wave-speed-angle relationship*

631 For each tested knee joint angle, PT shear-wave speed was normalised to the maximum shear-
632 wave speed obtained during the submaximal fixed-end reference contractions at the three target
633 knee joint angles. Following this, a second-order polynomial curve was fitted to the shear-wave
634 speed crank-arm angle data.

635

636 *Residual force enhancement*

637 rFE based on resultant torque ($rFE_{TQ}$) and shear-wave speed ($rFE_{WS}$) measurements were
638 calculated as the percent mean difference between the stretch-hold and fixed-end reference
639 contractions from 2.5 to 3.0 s after stretch (i.e. ~6 s after contraction onset) at the same target
640 knee joint angle. The 0.5-s interval to calculate rFE used here is in line with previous studies
641 (Hahn et al. 2010, 2012) and ensures that rFE was estimated during the isometric steady-state
642 following stretch.

643

644 *EMG activity*

645 Superficial quadriceps muscle activities and biceps femoris muscle activity during stretch-hold
646 contractions was quantified by taking the mean EMG RMS amplitude from 2.5-3 s after stretch.
647 Muscle activity during stretch-hold contractions was then compared with the time-matched
648 muscle activity during the fixed-end contractions. Mean EMG RMS values of VL, VM, RF and
649 the summed superficial quadriceps activity during stretch-hold and fixed-end contractions were
650 then normalised to the angle-specific maximum muscle activity recorded during the MVCs. To
651 determine the desired EMG levels that participants needed to match at the target knee joint
652 angles (i.e. short, long, and very long muscle lengths), we fitted a second-order polynomial
653 curve to the EMG-angle data from the MVCs at 30°, 70° and 110° crank-arm angle.

654

bioRxiv preprint doi: https://doi.org/10.1101/2022.02.11.480120; this version posted February 14, 2022. The copyright holder for this preprint (which was not certified by peer review) is the author/funder, who has granted bioRxiv a license to display the preprint in perpetuity. It is made available under a CC-BY 4.0 International license.



*Fascicle length and length changes*

VL fascicle lengths from each muscle length condition were initially calculated offline from the last image of each ultrasound recording using linear extrapolation to find the intersections between one representative fascicle and VL's superficial and deep aponeuroses. To reduce subjectivity of the fascicle length determination, the fascicle orientation was automatically determined by fitting a straight-line through user-selected feature points, and the aponeuroses were automatically determined using feature detection. Custom software was then used to track VL muscle fascicle length changes from the last to first ultrasound image by applying a Lucas-Kanade-Tomasi based affine optic flow algorithm. This algorithm is similar to the algorithm used by UltraTrack (Farris and Lichtwark 2016), except that it only tracks detected feature points (Shi and Tomasi 1994) across sequential images. To improve algorithm performance, the feature points were only detected from within a user-defined region of interest that spanned the image field of view and was located on VL's superficial aponeurosis and just above (i.e. 0.4 to 3.5 mm) VL's deep aponeurosis. Additionally, ultrasound recordings were downsampled from 150 to 30 fps as this resulted in less frame-to-frame fascicle length change underestimation.

To determine whether fascicle lengths were similar between the stretch-hold and fixed-end reference contractions, VL muscle fascicle length data was analysed during the same time interval as the torque and shear-wave-speed data. During stretch-hold contractions, the magnitude of fascicle stretch was determined from the start to end of fascicle lengthening 0.5 s before and after the dynamometer-imposed rotation. The start of fascicle lengthening was determined as the first time point when VL fascicle velocity was $\geq 0.05$ $mms^{-1}$, and the end of fascicle lengthening was determined as the last time point when VL fascicle velocity was $\geq 0.05$ $mms^{-1}$. VL fascicle stretch was then calculated by calculating the difference in fascicle length

bioRxiv preprint doi: https://doi.org/10.1101/2022.02.11.480120; this version posted February 14, 2022. The copyright holder for this preprint (which was not certified by peer review) is the author/funder, who has granted bioRxiv a license to display the preprint in perpetuity. It is made available under a CC-BY 4.0 International license.



at these two time points. VL fascicle velocity was determined by differentiating the filtered fascicle length data.

*Quadriceps force*

To estimate *in vivo* quadriceps muscle force, the resultant knee extension torques during the fixed-end contractions at short, long and very long muscle lengths were divided by the angle-specific PT moment arm from the recommended mean PT moment arm function provided by Bakenecker et al. 2019. The agreement between the estimated quadriceps muscle forces and squared patella tendon shear-wave speeds at each muscle length during the fixed-end contractions was then calculated as the mean percent difference between normalised quadriceps forces and normalised squared PT shear-wave speeds. Quadriceps forces and PT shear-wave speeds were normalised to their maximum during the fixed-end reference submaximal contractions over the three target joint angles.

**Statistics**

To detect outliers in muscle activity, shear-wave speed, torque or fascicle behaviour data in the stretch-hold or fixed-end reference conditions, a method based on a range of four around the median absolute deviation (MAD) was used (Leys et al. 2013). Two-way repeated-measures ANOVAs or mixed-effects analyses (only for datasets with missing values due to outliers) were performed to identify differences in summed superficial quadriceps muscle activity level, resultant knee extension torque, PT shear-wave speed, and absolute VL fascicle lengths between stretch-hold and fixed-end reference contractions across muscle lengths (contraction condition × muscle length). A two-way repeated-measures ANOVA was also used to identify differences in rFE between rFE methods ($rFE_{TQ}$ and $rFE_{WS}$) across muscle lengths (rFE determination method × muscle length). A one-way repeated-measures ANOVA was used to identify differences in VL fascicle stretch magnitudes across muscle lengths during the stretch-

bioRxiv preprint doi: https://doi.org/10.1101/2022.02.11.480120; this version posted February 14, 2022. The copyright holder for this preprint (which was not certified by peer review) is the author/funder, who has granted bioRxiv a license to display the preprint in perpetuity. It is made available under a CC-BY 4.0 International license.



hold contractions. Repeated-measures Pearson correlation coefficients were calculated to test the strength of the relationships between $rFE_{TQ}$ or $rFE_{WS}$ and VL fascicle stretch amplitudes or absolute VL fascicle lengths using the rmcorr package (Bakdash and Marusich 2017) in RStudio (v1.4.1717, 2021, Boston, USA). The alpha level was set at $p \leq 0.05$ and statistical analyses were performed using commercially-available software (GraphPad Prism 9, USA).

## Competing interests

The authors declare no competing interests.

## Authors' contribution

PB contributed to conception and design of the study, acquisition of data, data analysis and interpretation, and drafted the manuscript; TW contributed to conception and design of the study, data analysis and interpretation and revising the manuscript critically; DH contributed to conception and design of the study, data interpretation and revising the manuscript critically; BR contributed to conception and design of the study, data analysis and interpretation and revising the manuscript critically; all authors gave final approval for publication.

bioRxiv preprint doi: https://doi.org/10.1101/2022.02.11.480120; this version posted February 14, 2022. The copyright holder for this preprint (which was not certified by peer review) is the author/funder, who has granted bioRxiv a license to display the preprint in perpetuity. It is made available under a CC-BY 4.0 International license.



## References

Abbott BC, Aubert XM (1952) The force exerted by active striated muscle during and after change of length. The Journal of Physiology 117:77–86

Arampatzis A, Karamanidis K, de Monte G, et al (2004) Differences between measured and resultant joint moments during voluntary and artificially elicited isometric knee extension contractions. Clinical Biomechanics 19:277–283. https://doi.org/10.1016/j.clinbiomech.2003.11.011

Bakdash JZ, Marusich LR (2017) Repeated Measures Correlation. Front Psychol 8:456. https://doi.org/10.3389/fpsyg.2017.00456

Bakenecker P, Raiteri B, Hahn D (2019) Patella tendon moment arm function considerations for human vastus lateralis force estimates. Journal of Biomechanics 86:225–231. https://doi.org/10.1016/j.jbiomech.2019.01.042

Bakenecker P, Raiteri BJ, Hahn D (2020) Force enhancement in the human vastus lateralis is muscle-length-dependent following stretch but not during stretch. Eur J Appl Physiol 120:2597–2610. https://doi.org/10.1007/s00421-020-04488-1

Blank JL, Thelen DG, Allen MS, Roth JD (2022) Sensitivity of the shear wave speed-stress relationship to soft tissue material properties and fiber alignment. Journal of the Mechanical Behavior of Biomedical Materials 125:104964. https://doi.org/10.1016/j.jmbbm.2021.104964

Bullimore SR, Leonard TR, Rassier DE, Herzog W (2007) History-dependence of isometric muscle force: Effect of prior stretch or shortening amplitude. Journal of Biomechanics 40:1518–1524. https://doi.org/10.1016/j.jbiomech.2006.06.014

Cook CS, McDonagh MJ (1995) Force responses to controlled stretches of electrically stimulated human muscle-tendon complex. Experimental Physiology 80:477–490

de Campos D, Orssatto LBR, Trajano GS, et al (2021) Residual force enhancement in human skeletal muscles: A systematic review and meta-analysis. Journal of Sport and Health Science. https://doi.org/10.1016/j.jshs.2021.05.006

Edman KA, Elzinga G, Noble MI (1978) Enhancement of mechanical performance by stretch during tetanic contractions of vertebrate skeletal muscle fibres. The Journal of Physiology 281:139–155

Edman KA, Elzinga G, Noble MI (1982) Residual force enhancement after stretch of contracting frog single muscle fibers. The Journal of General Physiology 80:769–784. https://doi.org/10.1085/jgp.80.5.769

Farris DJ, Lichtwark GA (2016) UltraTrack: Software for semi-automated tracking of muscle fascicles in sequences of B-mode ultrasound images. Computer Methods and Programs in Biomedicine 128:111–118. https://doi.org/10.1016/j.cmpb.2016.02.016

Flann KL, LaStayo PC, McClain DA, et al (2011) Muscle damage and muscle remodeling: No pain, no gain? The Journal of Experimental biology 214:674–679. https://doi.org/10.1242/jeb.050112

Fukutani A, Misaki J, Isaka T (2017) Influence of Joint Angle on Residual Force Enhancement in Human Plantar Flexors. Frontiers in Physiology 8:234. https://doi.org/10.3389/fphys.2017.00234

Gandevia SC (2001) Spinal and supraspinal factors in human muscle fatigue. Physiological Reviews 81:1725–1789. https://doi.org/10.1152/physrev.2001.81.4.1725

Granzier HL, Burns DH, Pollack GH (1989) Sarcomere length dependence of the force-velocity relation in single frog muscle fibers. Biophysical Journal 55:499–507. https://doi.org/10.1016/S0006-3495(89)82843-7

bioRxiv preprint doi: https://doi.org/10.1101/2022.02.11.480120; this version posted February 14, 2022. The copyright holder for this preprint (which was not certified by peer review) is the author/funder, who has granted bioRxiv a license to display the preprint in perpetuity. It is made available under a CC-BY 4.0 International license.



765 Hahn D, Hoffman BW, Carroll TJ, Cresswell AG (2012) Cortical and spinal excitability during and
766 after lengthening contractions of the human plantar flexor muscles performed with maximal voluntary
767 effort. PloS One 7:e49907. https://doi.org/10.1371/journal.pone.0049907

768 Hahn D, Riedel TN (2018) Residual force enhancement contributes to increased performance during
769 stretch-shortening cycles of human plantar flexor muscles in vivo. Journal of Biomechanics 77:190–
770 193. https://doi.org/10.1016/j.jbiomech.2018.06.003

771 Hahn D, Seiberl W, Schmidt S, et al (2010) Evidence of residual force enhancement for multi-joint leg
772 extension. Journal of biomechanics 43:1503–1508. https://doi.org/10.1016/j.jbiomech.2010.01.041

773 Hahn D, Seiberl W, Schwirtz A (2007) Force enhancement during and following muscle stretch of
774 maximal voluntarily activated human quadriceps femoris. European Journal of Applied Physiology
775 100:701–709. https://doi.org/10.1007/s00421-007-0462-3

776 Hermens HJ, Freriks B, Disselhorst-Klug C, Rau G (2000) Development of recommendations for
777 SEMG sensors and sensor placement procedures. Journal of Electromyography and Kinesiology
778 10:361–374. https://doi.org/10.1016/S1050-6411(00)00027-4

779 Hisey B, Leonard TR, Herzog W (2009) Does residual force enhancement increase with increasing
780 stretch magnitudes? Journal of Biomechanics 42:1488–1492.
781 https://doi.org/10.1016/j.jbiomech.2009.03.046

782 Keuler EM, Loegering IF, Martin JA, et al (2019) Shear Wave Predictions of Achilles Tendon
783 Loading during Human Walking. Scientific Reports 9:1–9. https://doi.org/10.1038/s41598-019-49063-
784 7

785 Kuervers EJ, Firminger CR, Edwards WB (2021) Effect of Knee Angle and Quadriceps Muscle Force
786 on Shear-Wave Elastography Measurements at the Patellar Tendon. Ultrasound Med Biol 47:2167–
787 2175. https://doi.org/10.1016/j.ultrasmedbio.2021.03.031

788 Lee H-D, Herzog W (2002) Force enhancement following muscle stretch of electrically stimulated and
789 voluntarily activated human adductor pollicis. The Journal of Physiology 545:321–330.
790 https://doi.org/10.1113/jphysiol.2002.018010

791 Lee HD, Herzog W, Leonard T (2001) Effects of cyclic changes in muscle length on force production
792 in in-situ cat soleus. Journal of Biomechanics 34:979–987. https://doi.org/10.1016/S0021-
793 9290(01)00077-X

794 Leonard TR, DuVall M, Herzog W (2010) Force enhancement following stretch in a single sarcomere.
795 American journal of physiology Cell physiology 299:C1398-401.
796 https://doi.org/10.1152/ajpcell.00222.2010

797 Leys C, Ley C, Klein O, et al (2013) Detecting outliers: Do not use standard deviation around the
798 mean, use absolute deviation around the median. Journal of Experimental Social Psychology 49:764–
799 766. https://doi.org/10.1016/j.jesp.2013.03.013

800 Maganaris CN, Baltzopoulos V, Sargeant AJ (2002) Repeated contractions alter the geometry of
801 human skeletal muscle. Journal of Applied Physiology 93:2089–2094.
802 https://doi.org/10.1152/japplphysiol.00604.2002

803 Martin JA, Brandon SCE, Keuler EM, et al (2018) Gauging force by tapping tendons. Nature
804 Communications 9:1592. https://doi.org/10.1038/s41467-018-03797-6

805 Martin JA, Kindig MW, Stender CJ, et al (2020) Calibration of the shear wave speed-stress
806 relationship in in situ Achilles tendons using cadaveric simulations of gait and isometric contraction.
807 Journal of Biomechanics 106:109799. https://doi.org/10.1016/j.jbiomech.2020.109799

bioRxiv preprint doi: https://doi.org/10.1101/2022.02.11.480120; this version posted February 14, 2022. The copyright holder for this preprint (which was not certified by peer review) is the author/funder, who has granted bioRxiv a license to display the preprint in perpetuity. It is made available under a CC-BY 4.0 International license.



Morgan DL (1990) New insights into the behavior of muscle during active lengthening. Biophysical Journal 57:209–221. https://doi.org/10.1016/S0006-3495(90)82524-8

Nisell R (1985) Mechanics of the knee. A study of joint and muscle load with clinical applications. Acta orthopaedica Scandinavica 216:1–42

Oskouei AE, Herzog W (2005) Observations on force enhancement in submaximal voluntary contractions of human adductor pollicis muscle. J Appl Physiol (1985) 98:2087–2095. https://doi.org/10.1152/japplphysiol.01217.2004

Oskouei AE, Herzog W (2006) The dependence of force enhancement on activation in human adductor pollicis. European Journal of Applied Physiology 98:22–29. https://doi.org/10.1007/s00421-006-0170-4

Paternoster FK, Holzer D, Arlt A, et al (2021) Residual force enhancement in humans: Is there a true non-responder? Physiological Reports 9:e14944. https://doi.org/10.14814/phy2.14944

Pinnell RAM, Mashouri P, Mazara N, et al (2019) Residual force enhancement and force depression in human single muscle fibres. J Biomech 91:164–169. https://doi.org/10.1016/j.jbiomech.2019.05.025

Pinniger GJ, Cresswell AG (2007) Residual force enhancement after lengthening is present during submaximal plantar flexion and dorsiflexion actions in humans. Journal of applied physiology (Bethesda, Md : 1985) 102:18–25. https://doi.org/10.1152/japplphysiol.00565.2006

Power GA, Makrakos DP, Rice CL, Vandervoort AA (2013) Enhanced force production in old age is not a far stretch: An investigation of residual force enhancement and muscle architecture. Physiological Reports 1:e00004. https://doi.org/10.1002/phy2.4

Raiteri BJ, Hahn D (2019) A reduction in compliance or activation level reduces residual force depression in human tibialis anterior. Acta Physiologica 225:. https://doi.org/10.1111/apha.13198

Rassier DE, Herzog W (2005) Relationship between force and stiffness in muscle fibers after stretch. Journal of Applied Physiology 99:1769–1775. https://doi.org/10.1152/japplphysiol.00010.2005

Sarvazyan AP, Urban MW, Greenleaf JF (2013) Acoustic Waves in Medical Imaging and Diagnostics. Ultrasound in Medicine & Biology 39:1133–1146. https://doi.org/10.1016/j.ultrasmedbio.2013.02.006

Seiberl W, Hahn D, Herzog W, Schwirtz A (2012) Feedback controlled force enhancement and activation reduction of voluntarily activated quadriceps femoris during sub-maximal muscle action. Journal of Electromyography and Kinesiology : Official Journal of the International Society of Electrophysiological Kinesiology 22:117–123. https://doi.org/10.1016/j.jelekin.2011.10.010

Seiberl W, Power GA, Hahn D (2015) Residual force enhancement in humans: Current evidence and unresolved issues. Journal of Electromyography and Kinesiology : official Journal of the International Society of Electrophysiological Kinesiology 25:571–580. https://doi.org/10.1016/j.jelekin.2015.04.011

Sharifnezhad A, Marzilger R, Arampatzis A (2014) Effects of load magnitude, muscle length and velocity during eccentric chronic loading on the longitudinal growth of the vastus lateralis muscle. The Journal of Experimental Biology 217:2726–2733. https://doi.org/10.1242/jeb.100370

Shi J, Tomasi C (1994) Good Features to Track. Proceedings of IEEE Conference on Computer Vision and Pattern Recognition, pp. 593-600, https://doi.org/10.1109/CVPR.1994.323794.

Shim J, Garner B (2012) Residual force enhancement during voluntary contractions of knee extensors and flexors at short and long muscle lengths. Journal of Biomechanics 45:913–918. https://doi.org/10.1016/j.jbiomech.2012.01.026

Tilp M, Steib S, Herzog W (2009) Force-time history effects in voluntary contractions of human tibialis anterior. European Journal of Applied Physiology 106:159–166.

bioRxiv preprint doi: https://doi.org/10.1101/2022.02.11.480120; this version posted February 14, 2022. The copyright holder for this preprint (which was not certified by peer review) is the author/funder, who has granted bioRxiv a license to display the preprint in perpetuity. It is made available under a CC-BY 4.0 International license.



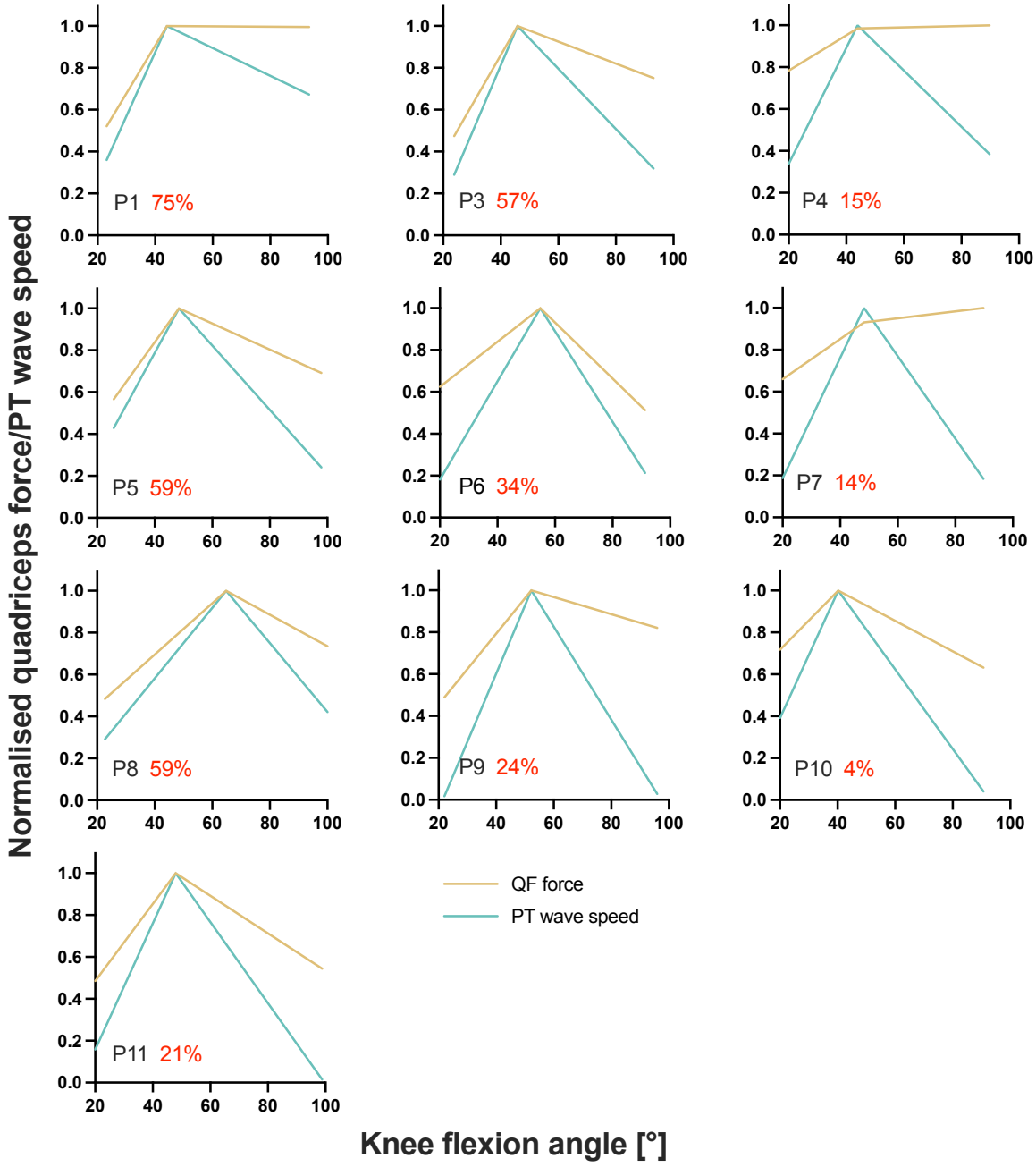
https://doi.org/10.1007/s00421-009-1006-9

Tsaopoulos DE, Baltzopoulos V, Richards PJ, Maganaris CN (2007) In vivo changes in the human patellar tendon moment arm length with different modes and intensities of muscle contraction. Journal of Biomechanics 40:3325–3332. https://doi.org/10.1016/j.jbiomech.2007.05.005

bioRxiv preprint doi: https://doi.org/10.1101/2022.02.11.480120; this version posted February 14, 2022. The copyright holder for this preprint (which was not certified by peer review) is the author/funder, who has granted bioRxiv a license to display the preprint in perpetuity. It is made available under a CC-BY 4.0 International license.



856 *Supplementary Material*




857

858 Figure 1. Individual normalised quadriceps-force (QF)-angle and patellar tendon shear-wave speed-($PT_{WS}$)-angle
859 relationships determined from the fixed-end reference ramp contractions at the short, long, and very long muscle
860 lengths from part 1 of the experiment. The average agreement across muscle lengths ($PT_{WS}$ – QF / mean of $PT_{WS}$
861 and QF) between normalised QFs and PT shear-wave speeds is indicated as a percentage for every participant,
862 where red font has been used to highlight instances of less than 90% agreement. P2 had to be excluded from this
863 analysis due to missing marker data.

864

865

bioRxiv preprint doi: https://doi.org/10.1101/2022.02.11.480120; this version posted February 14, 2022. The copyright holder for this preprint (which was not certified by peer review) is the author/funder, who has granted bioRxiv a license to display the preprint in perpetuity. It is made available under a CC-BY 4.0 International license.



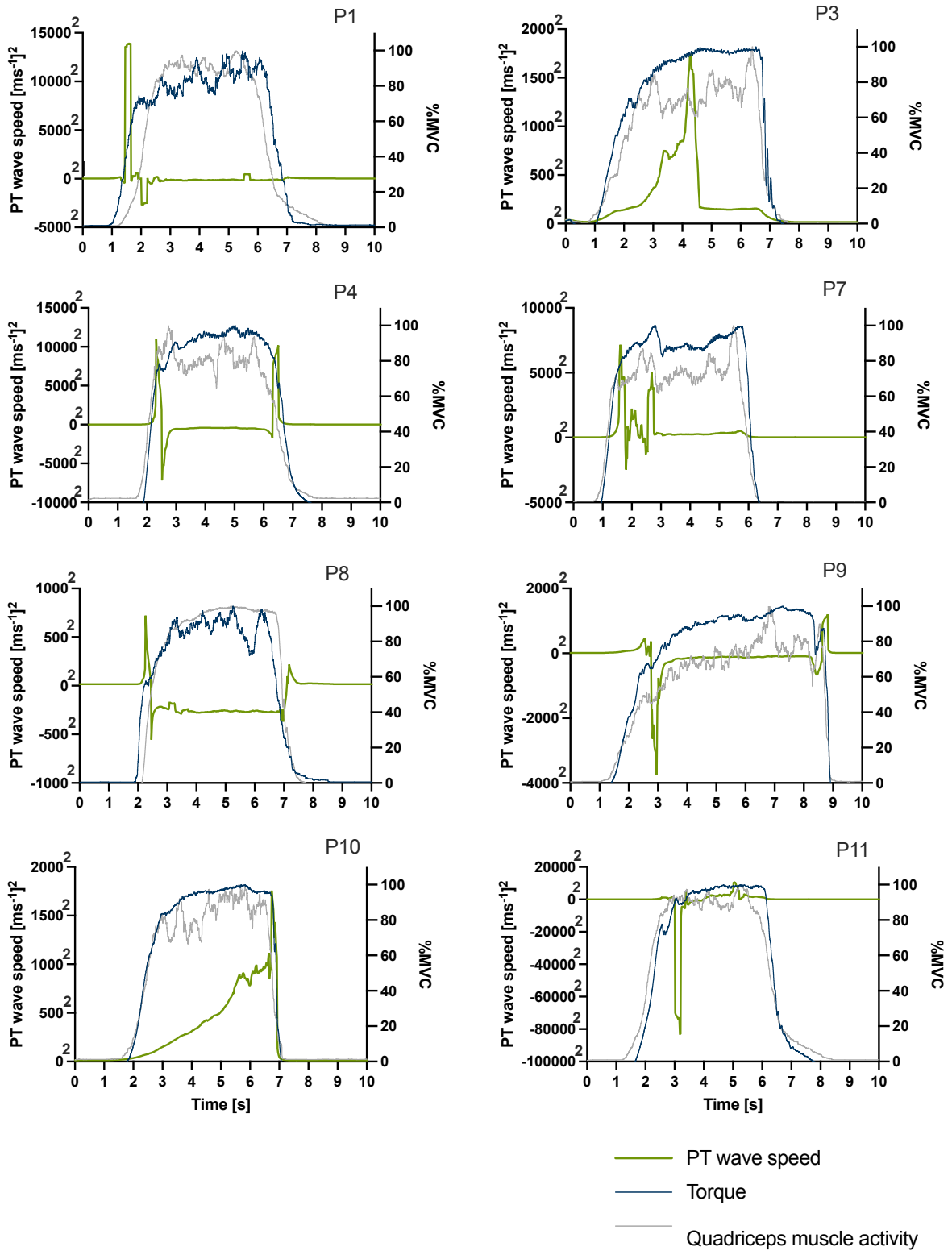
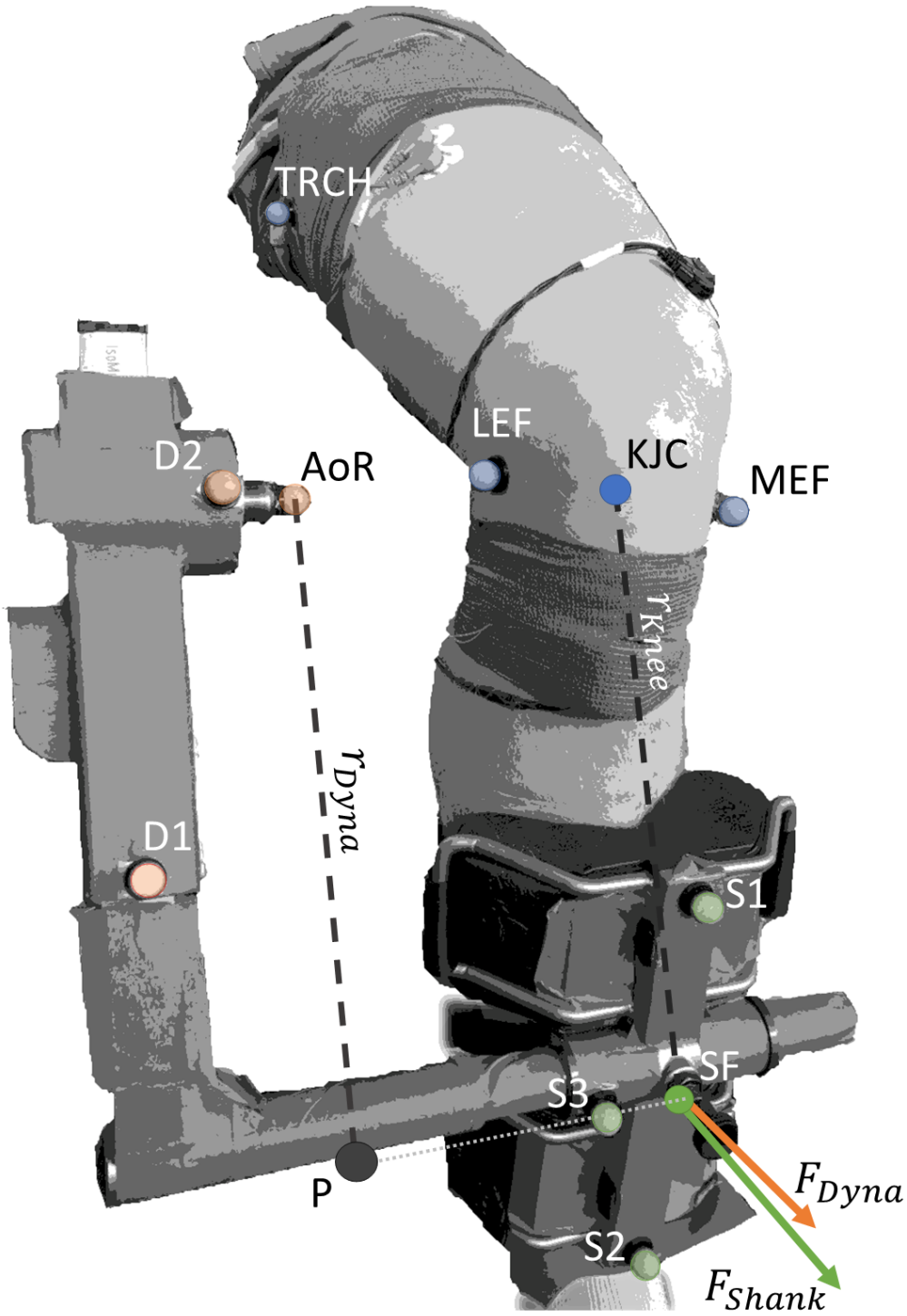



Figure 2. Individual patellar tendon (PT) shear-wave-speed-time (green), knee extension torque-time (blue), and summed quadriceps muscle activity level-time traces (grey) during maximum voluntary fixed-end reference contractions at a 70° crank arm angle from the first part of the experiment. Knee extension torques and the summed quadriceps muscle activities (shown on the right y-axis) were normalized to maximum knee extension torques and maximum summed quadriceps muscle activity level, respectively. P2 was excluded due to missing marker data.

bioRxiv preprint doi: https://doi.org/10.1101/2022.02.11.480120; this version posted February 14, 2022. The copyright holder for this preprint (which was not certified by peer review) is the author/funder, who has granted bioRxiv a license to display the preprint in perpetuity. It is made available under a CC-BY 4.0 International license.



872



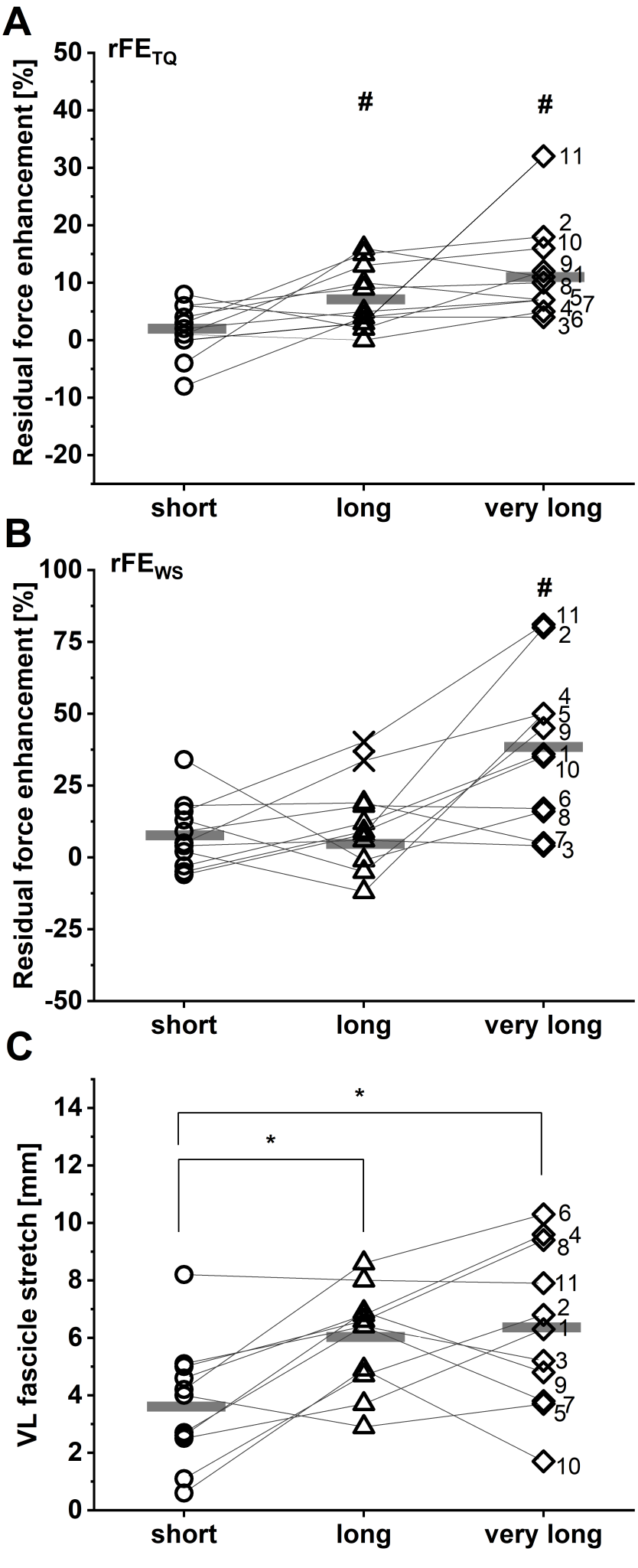

873

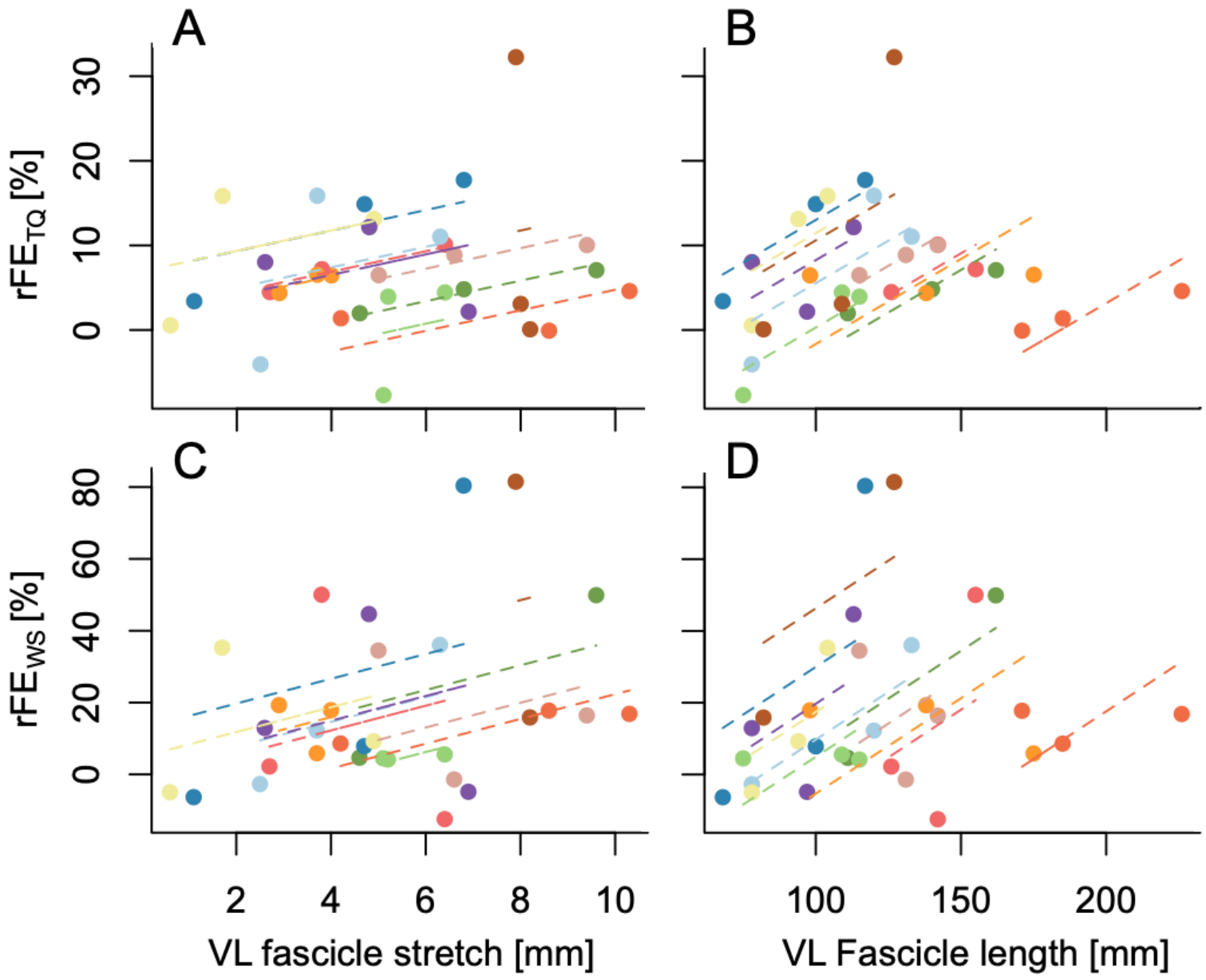
874 Figure 3. Resultant torque was calculated by multiplying the force acting at the shank ($F_{Shank}$) by the external
875 moment arm to the knee ($r_{Knee}$). $F_{Shank}$ acted at the midpoint of the pad attached to the shank and $r_{Knee}$ was the
876 perpendicular distance from the line of action of $F_{Shank}$ to the knee joint center (KJC). $F_{Shank}$ was calculated by

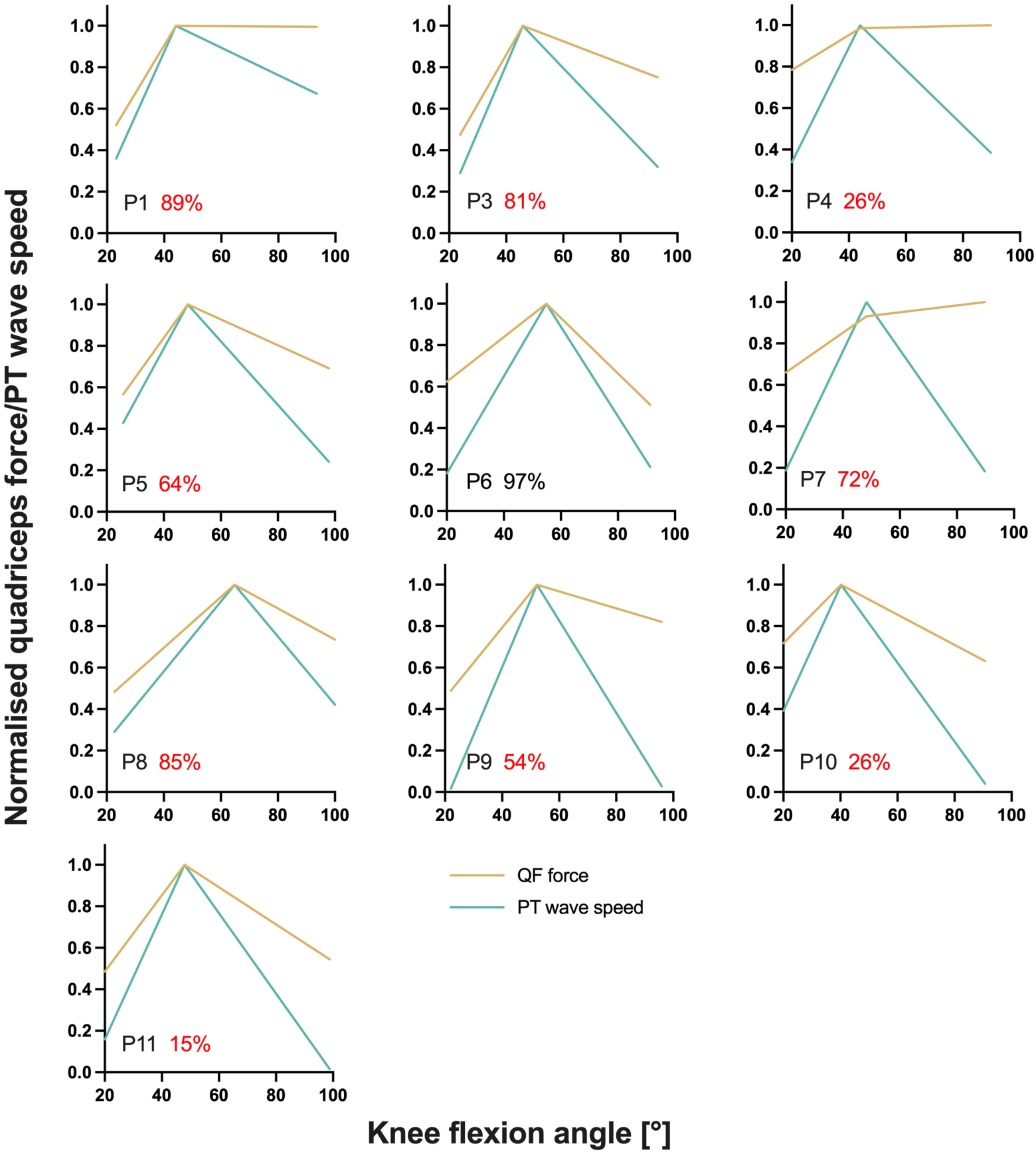
bioRxiv preprint doi: https://doi.org/10.1101/2022.02.11.480120; this version posted February 14, 2022. The copyright holder for this preprint (which was not certified by peer review) is the author/funder, who has granted bioRxiv a license to display the preprint in perpetuity. It is made available under a CC-BY 4.0 International license.

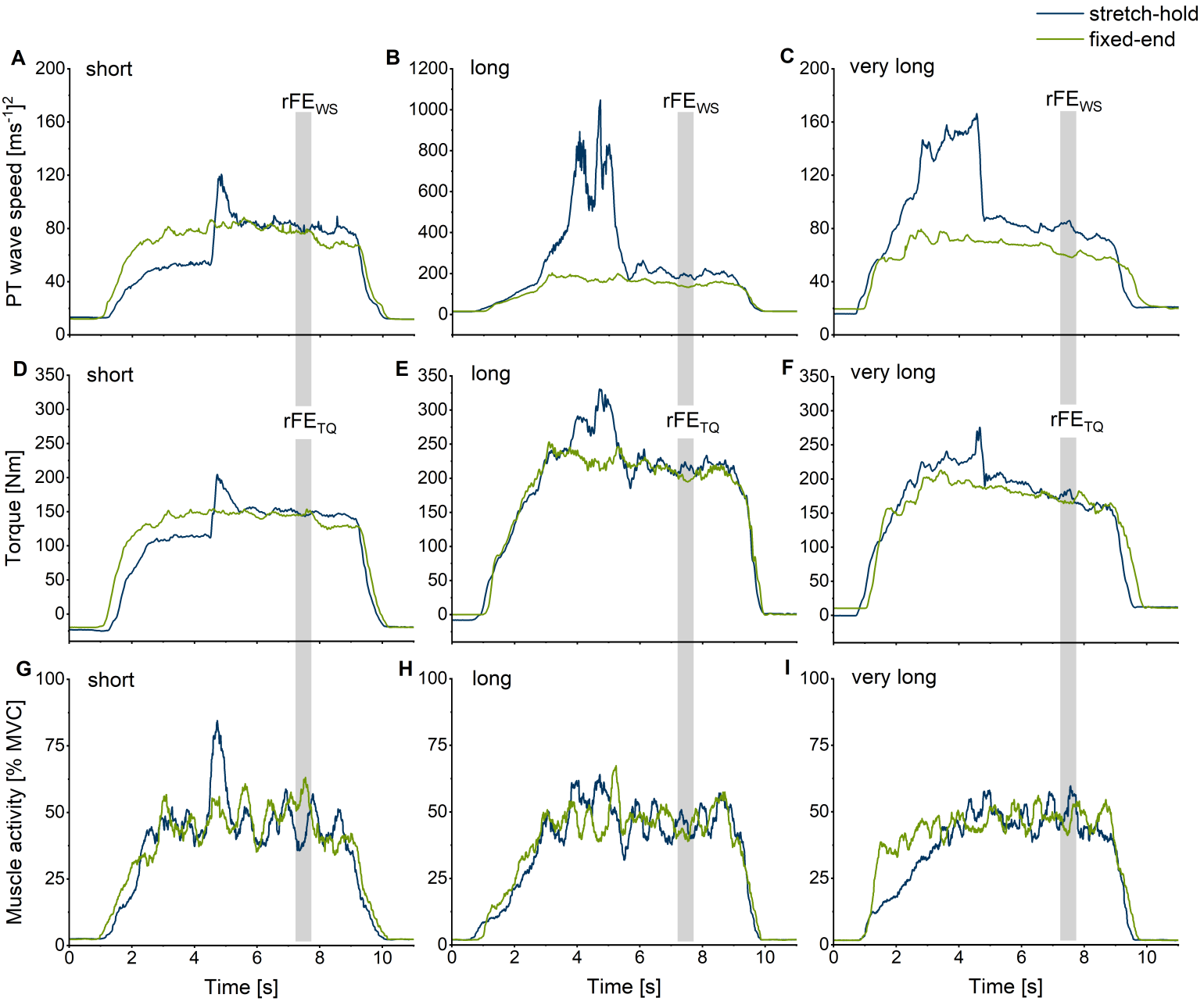


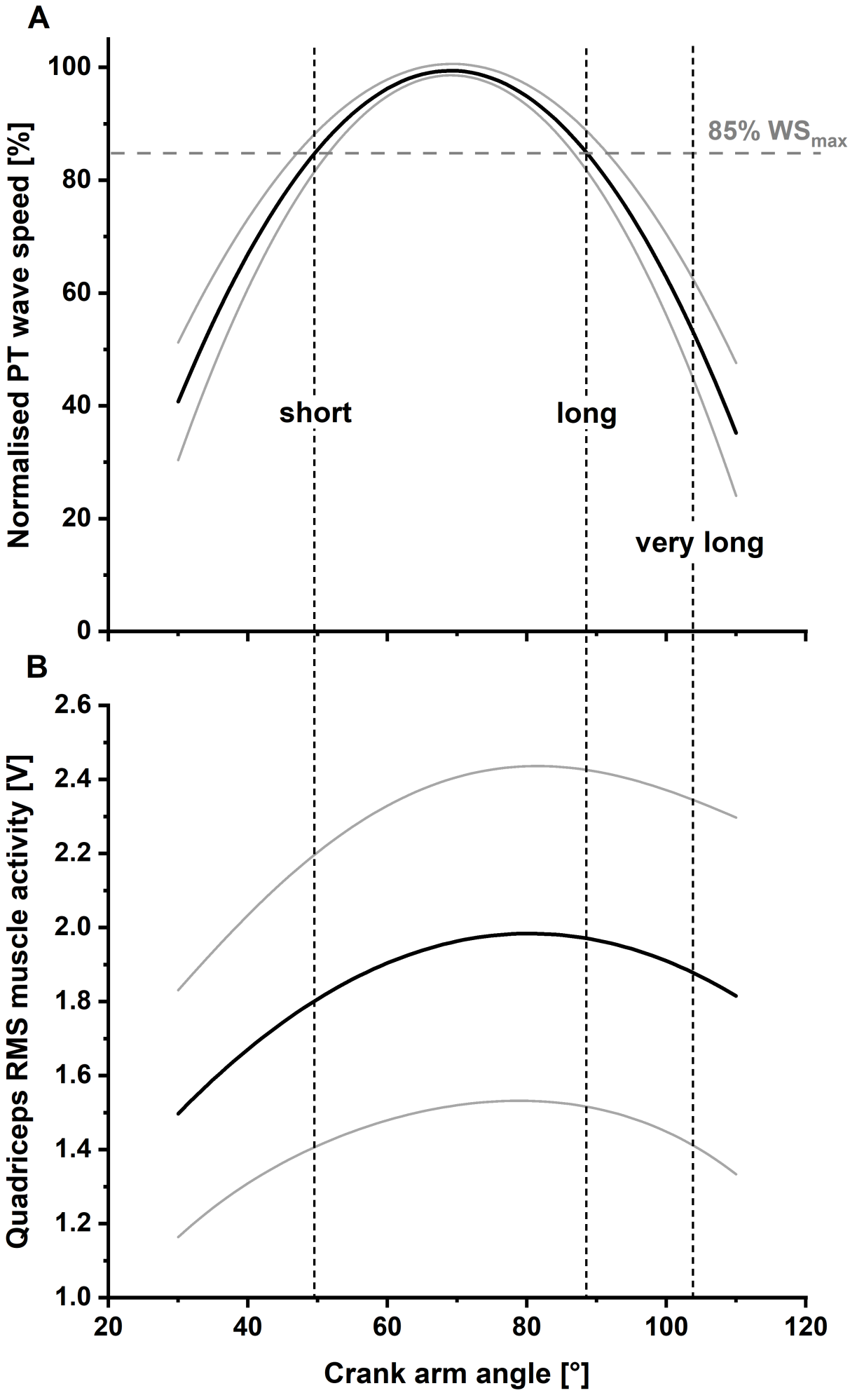
dividing the calculated dynamometer force ($F_{Dyna}$) by the cosine of the angle between the two force vectors, $F_{Shank}$ and $F_{Dyna}$, whose respective directions were defined by the normal vectors of the planes formed by Shank Maker 1 (S1), S2 and S3, and Dynamometer Marker 1 (D1), D2 and the dynamometer's axis of rotation (AoR). $F_{Dyna}$ was calculated by dividing the measured torque at the dynamometer AoR by the external moment arm of the dynamometer ($r_{Dyna}$). $r_{Dyna}$ was calculated as the distance between P and AoR. P was defined as the shortest distance between the projection of AoR onto the vector formed by S3 and the midpoint of the pad attached to the shank (SF). Transparent colored markers indicate captured markers, whereas solid marker KJC was calculated as the midpoint between the lateral and medial epicondyles of the femur (LEF and MEF, respectively) and solid marker SF was calculated as the midpoint between S1 and S2.

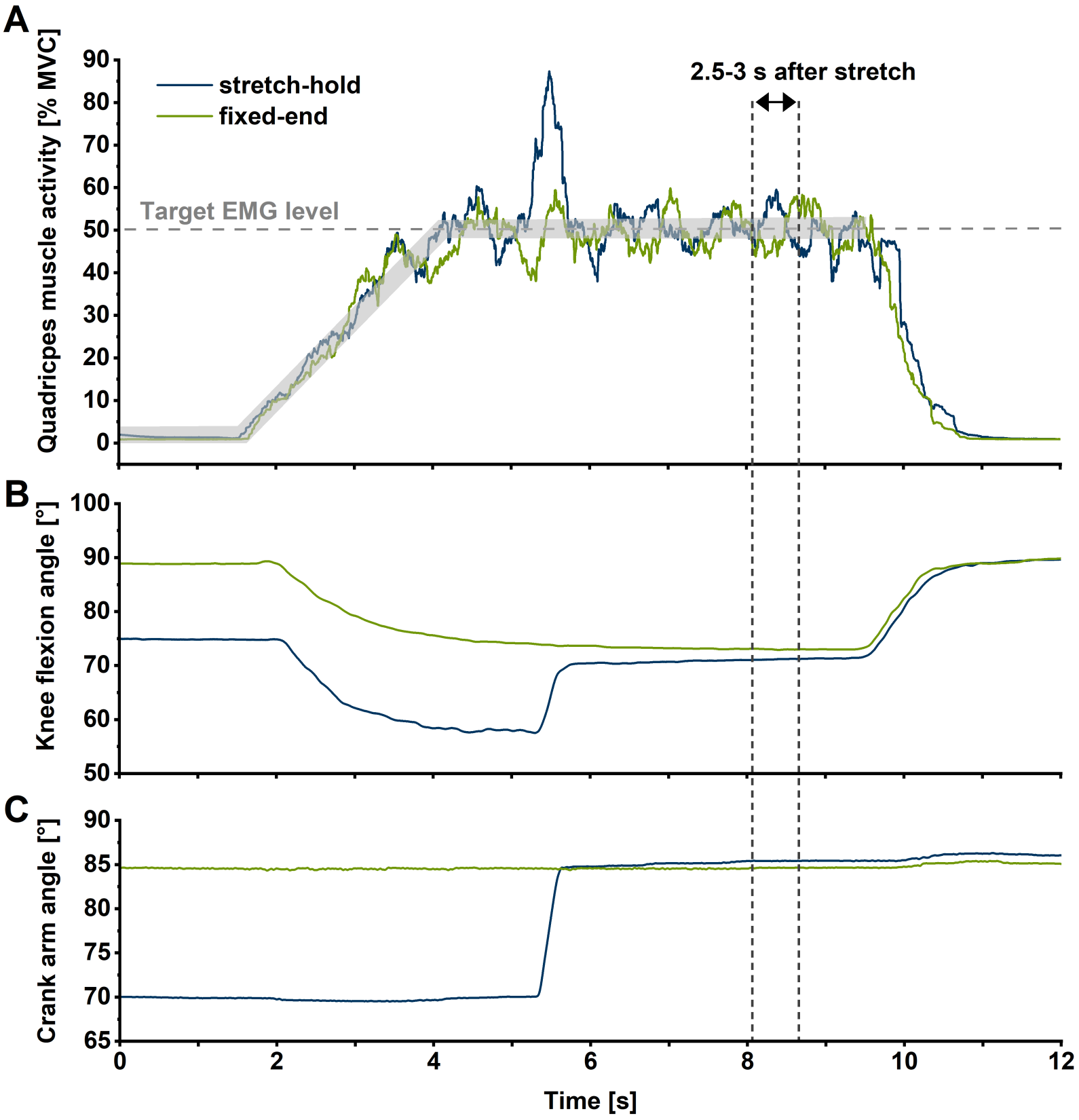

A
rFE_TQ
Residual force enhancement [%]
50
40
30
20
10
0
-10
-20
#
#
11
2
10
9
1
8
5
7
4
3
6
short
long
very long
B
rFE_WS
Residual force enhancement [%]
100
75
50
25
0
-25
-50
#
11
2
4
5
9
1
10
6
8
7
3
short
long
very long
C
VL fascicle stretch [mm]
14
12
10
8
6
4
2
0
*
*
6
8
4
11
2
1
3
9
7
5
10
short
long
very long

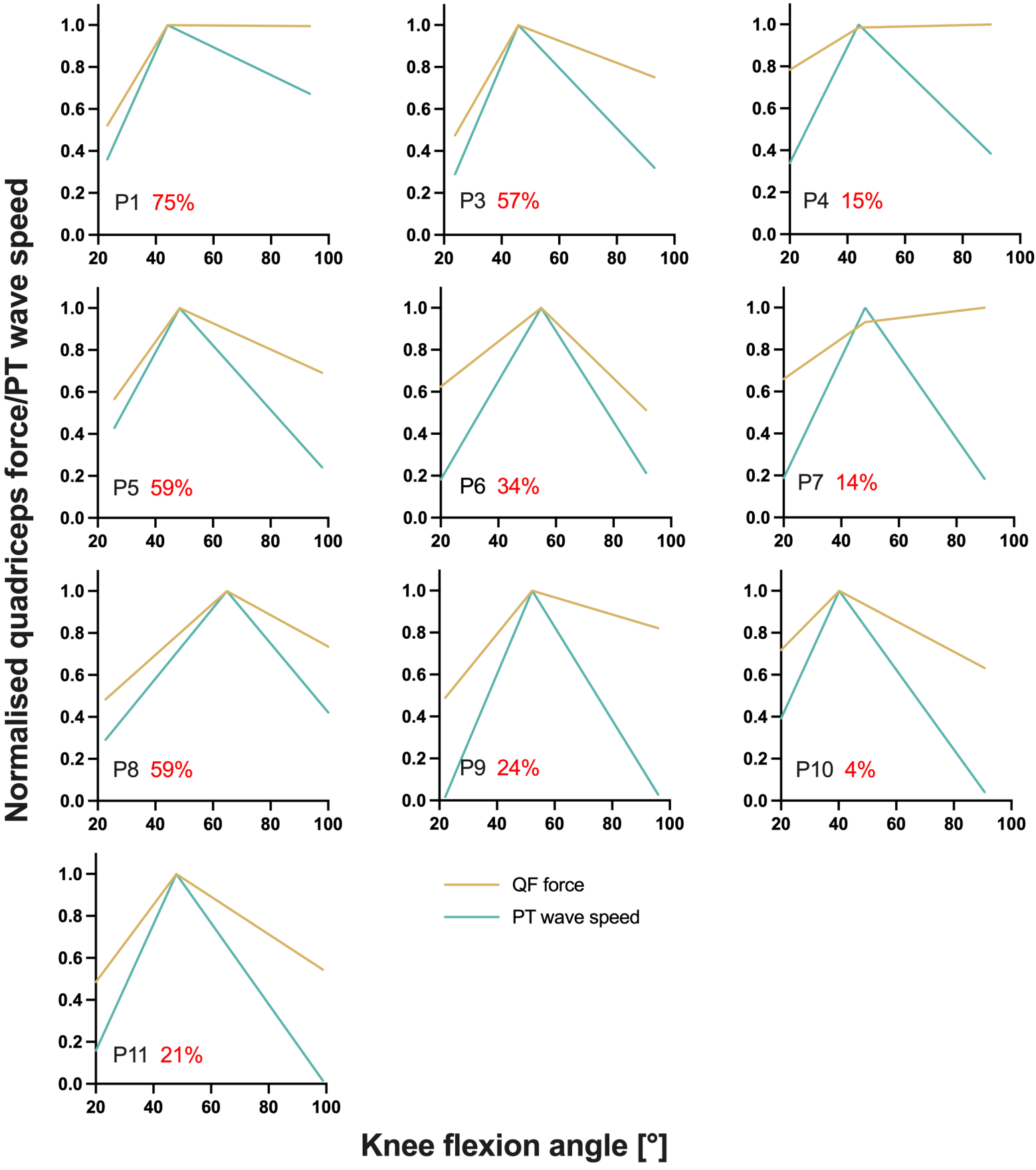

A
B
C
D
rFE_TQ [%]
rFE_WS [%]
0
10
20
30
0
20
40
60
80
2
4
6
8
10
100
150
200
VL fascicle stretch [mm]
VL Fascicle length [mm]

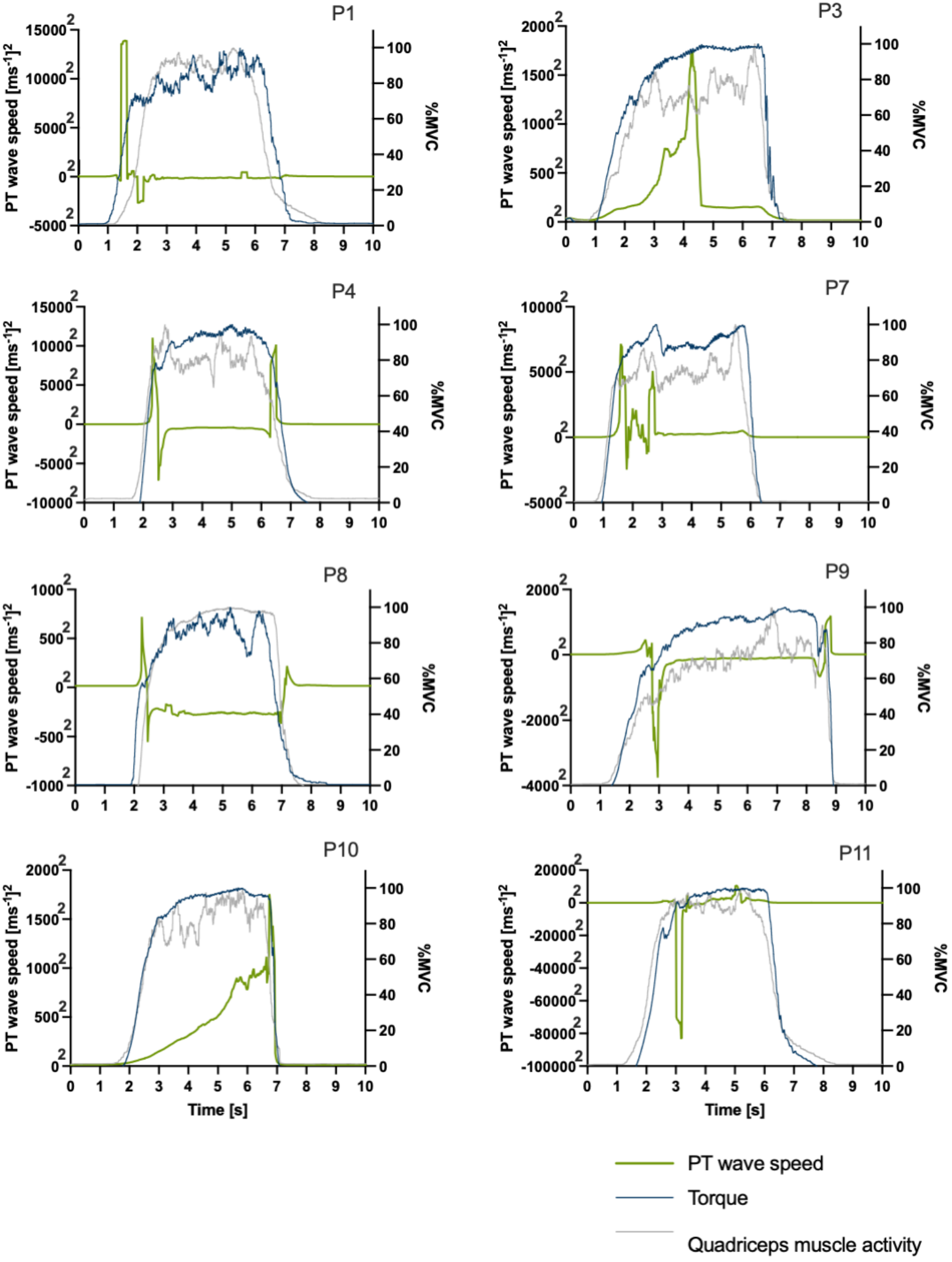

Normalised quadriceps force/PT wave speed
P1 89%
P3 81%
P4 26%
P5 64%
P6 97%
P7 72%
P8 85%
P9 54%
P10 26%
P11 15%
QF force
PT wave speed
Knee flexion angle [°]

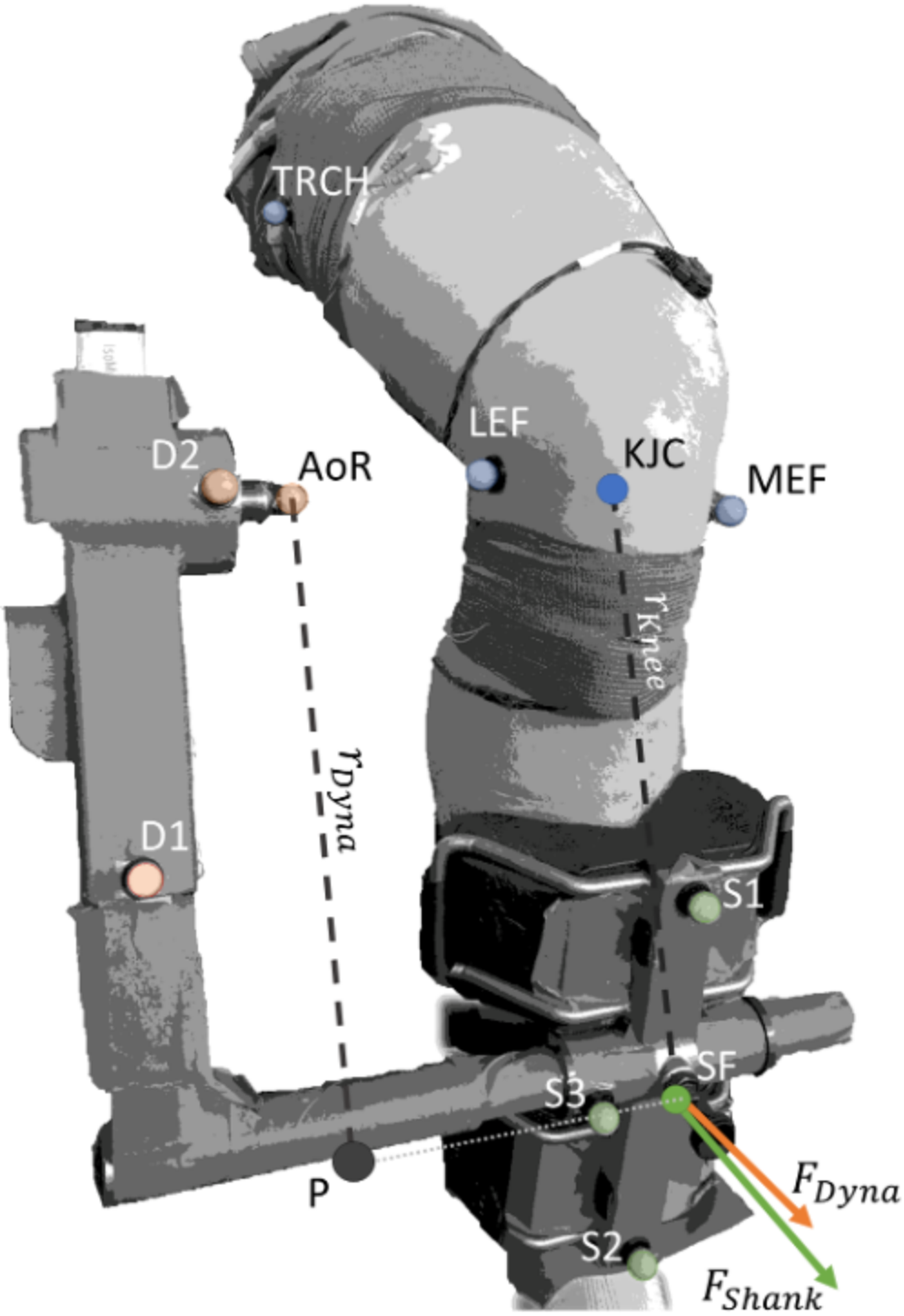

stretch-hold
fixed-end
A
short
rFE_WS
B
long
rFE_WS
C
very long
rFE_WS
PT wave speed [ms^-1]^2
D
short
rFE_TQ
E
long
rFE_TQ
F
very long
rFE_TQ
Torque [Nm]
G
short
H
long
I
very long
Muscle activity [% MVC]
Time [s]
Time [s]
Time [s]


A
Normalised PT wave speed [%]
100
80
60
40
20
0
85% WSmax
short
long
very long
B
Quadriceps RMS muscle activity [V]
2.6
2.4
2.2
2.0
1.8
1.6
1.4
1.2
1.0
20
40
60
80
100
120
Crank arm angle [°]


A
Quadricpes muscle activity [% MVC]
90
80
70
60
50
40
30
20
10
0
stretch-hold
fixed-end
2.5-3 s after stretch
Target EMG level
B
Knee flexion angle [°]
100
90
80
70
60
50
C
Crank arm angle [°]
90
85
80
75
70
65
0
2
4
6
8
10
12
Time [s]


Normalised quadriceps force/PT wave speed
P1 75%
P3 57%
P4 15%
P5 59%
P6 34%
P7 14%
P8 59%
P9 24%
P10 4%
P11 21%
QF force
PT wave speed
Knee flexion angle [°]


P1
P3
P4
P7
P8
P9
P10
P11
PT wave speed [ms-1]2
%MVC
Time [s]
PT wave speed
Torque
Quadriceps muscle activity


TRCH
LEF
KJC
MEF
D2
AoR
D1
$r_{Dyna}$
$r_{Knee}$
S1
SF
S3
P
S2
$F_{Dyna}$
$F_{Shank}$